Hairpin turn dislocations in two-dimensional smectic phases of long semiflexible polymers

Leonardo Golubović
Department of Physics, West Virginia University, Morgantown, West Virginia 26506-6315
(Received 26 June 2001; published 7 November 2001)

We elucidate hairpin turn dislocations in two-dimensional smectic phases of long semi-flexible polymers. We discuss hairpin shapes, sizes, and free energies. We find that hairpin dislocation core may be, under some circumstances, substantially bigger than the smectic period size. Such hairpin dislocations are accompanied by large voids that are stable equilibrium structures with sizes determined by a competition of the polymer bending elasticity and smectic bulk elasticity. The large size of hairpin voids is associated with a low hairpin energy, much smaller than anticipated before. The actual hairpin shape, size, and energy are all qualitatively sensitive to the detailed nature of smectics. We document this by considering hairpin dislocations in lyotropic smectics (systems stabilized by repulsion between polymers, with a positive osmotic pressure) and in thermotropic smectics (systems stable even at zero osmotic pressure, with a preferred distance between semiflexible molecules). We discuss in detail hairpin dislocations in lyotropic sterically stabilized Smectics as well as in DNA-cationic lipid complexes. We elucidate the extinction of hairpin dislocations by annihilations with polymer end points. In lyotropic smectics, rates of these processes are shown to be limited by sluggish reptation of semiflexible molecules, as well as by substantial energy barriers.

DOI: 10.1103/PhysRevE.64.061901 PACS number(s): 87.15.−v, 61.30.Jf, 82.70.Kj

I. INTRODUCTION

Over the past few years, there has been an increased experimental and theoretical interest in structural properties of two-dimensional (2D) smectic-*A* phases [1,2]. In part, it has been stimulated by the recent discovery of such a phase of long DNA molecules intercalated between lipid membranes in DNA-cationic-lipid complexes [3–8]. In these systems, long semiflexible DNA molecules form stacks of one-dimensional smectic layers that are low-dimensional analogs of lamellar fluid membrane phases and other three-dimensional smectic-*A* phases, [9–13]. As discussed by Toner and Nelson [1], and by this author and Wang [2], 2D smectics have only a short-range positional order, in part, because of strong thermal fluctuations of smectic displacements (undulations) that diverge as power laws of the 2D system size. Moreover, in contrast to 3D smectics-*A*, in 2D smectics, dislocations are generally free and turn the smectic state into a nematic phase at large length scales [1]. Crossover length scale ξ_d between the smectic and nematic regime is essentially the average distance between the dislocations that form nearly ideal gas at low-temperatures T. This length scale,

$$\xi_d \sim a \exp(E_D/2k_BT), \tag{1.1}$$

crucially depends on the dislocation free energy E_D, [1]. In Eq. (1.1), a signifies the smectic phase period.

In 2D smectic phases of semiflexible polymers, the dislocations are either end points of these long molecules or their hairpinlike turns, see Fig. 1 [6–8]. In this paper, we elucidate hairpin turn dislocations in 2D smectic phases of long semiflexible polymers, such as DNA molecules adsorbed on a smooth substrate or intercalated between lipid membranes in DNA-cationic-lipid complexes. We discuss hairpin shapes, sizes, and their free energies ξ_d. We find that the hairpin turns may be, under some circumstances, substantially larger than the smectic period size. Such hairpin turns are accompanied by large voids somewhat similar to the Griffith-size lenticular fractures of smectics discussed by de Gennes, [14]. In contrast to fractures, hairpin voids are stable equilibrium structures with sizes determined by a subtle competition between the smectic bulk elasticity and bending elasticity of the semiflexible polymer in the core of hairpin dislocations, see Fig. 1. Hairpin dislocations with large voids are shown here to have relatively low free energies. They are significantly smaller than anticipated in some earlier simple estimates that equate the vertical size of the hairpin D with the size of the period of the smectic a [see Fig. 1]: With the assumption $D=a$, and, furthermore, by assuming that the hairpin energy $E_{\rm hp}$ is mostly the bending energy of the highly curved turn that the semiflexible polymer makes in the core of the dislocation, one easily obtains the estimate,

$$E_{\rm hp}=\frac{\pi\kappa}{a}. \tag{1.2}$$

Here, κ is the semiflexible polymer bending constant, whereas the polymer turn section is assumed to be a semicircle of the diameter a. By Eq. (1.2),

$$\frac{E_{\rm hp}}{2k_BT}=\frac{\pi\xi_p}{4a}, \tag{1.3}$$

where $\xi_p=2\kappa/k_BT$ is the semiflexible polymer persistence length. Commonly, $\xi_p \gg a$, and thus, the hairpin dislocation energy-temperature ratio is large, yielding, by Eq. (1.1), a large separation between hairpin dislocations in thermodynamic equilibrium. The problem with the above estimates is in the *ad hoc* assumption that $D\approx a$. In principle, hairpin may relax the above large bending energy simply by expanding to a size D bigger than a. This expansion, however, causes a long-range elastic distortion of the surrounding smectic medium, see Fig. 1. Eventually, the hairpin size and

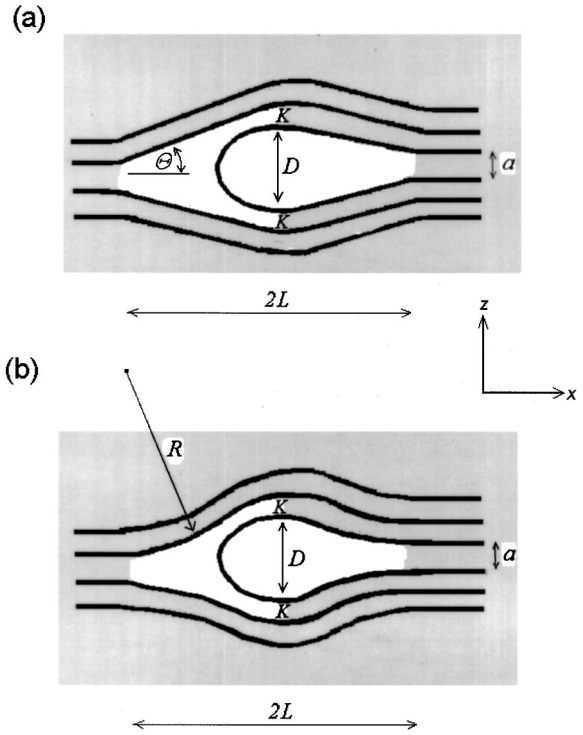

FIG. 1. Hairpin-turn dislocation in two-dimensional smectic phases of long flexible polymers. White areas (of the lateral size $2L$) are two wedge-shaped voids in the dislocation core region. The smectic medium is the gray area. In the core of the dislocation, between the contact points *K*, there is a highly curved polymer section of the linear size *D*, the *turn*. (a) depicts a hairpin dislocation in smectics at *zero* external pressure that are stabilized by intermolecular potentials assuming minimum at the preferred distance *a*, as in typical thermotropic smectics. In this case, interfaces between hairpin voids (white) and the smectic elastic medium (gray) are nearly straight lines making a finite angle θ with respect to smectic layer equilibrium direction. (b) depicts a hairpin dislocation in a smectic with purely repulsive interactions between semiflexible polymers, as in typical lyotropic smectics. For this case, a finite smectic period *a* is stabilized by a *positive* osmotic pressure of the smectic medium. In its presence, interfaces between voids (white) and the smectic medium (gray) curve and become nearly circular sections of the radius *R*.

energy will be determined by a competition of the smectic medium energy cost and the polymer bending energy cost. We study this competition throughout this paper.

Hairpin shapes, sizes and energies are shown here to be *qualitatively* sensitive to the detailed nature of smectic materials. We document this by considering two major classes of smectics, thermotropic and lyotropic smectics-*A*, see Fig. 1. We consider typical thermotropic smectics-*A* that are stable even at zero external isotropic pressure, due to having intermolecular potentials with a minimum at a preferred distance between semiflexible polymers. In these materials, at zero pressure, interfaces between hairpin voids and the smectic medium are nearly straight lines, as depicted in Fig. 1(a). We also consider hairpins in typical lyotropic smectics-*A*, stabilized by a repulsion between polymers causing a positive osmotic pressure. Here, the interfaces between hairpin voids and the smectic medium are nearly circular sections, as depicted in Fig. 1(b). For both the thermotropic and the lyotropic 2D smectics, we obtain hairpin dislocation sizes and energies. These quantities were related to basic materials properties, such as the smectic penetration length λ, the size of the smectic phase period *a*, and the semiflexible polymer persistence length ξ_p. Qualitative forms of these relations are found to be different for lyotropic and thermotropic smectic materials, as detailed in Secs. II to IV. In Sec. V, we apply our results for lyotropic smectics to entropically stabilized systems of long semiflexible polymers with purely hard-core repulsion [15–17], that are 2D analogs of fluid membrane lamellar phases stabilized by steric entropy [18,9–11]. We also discuss, in Sec. VI, hairpin-turn dislocations in smectics stabilized by electrostatic repulsion of the form appropriate for the quasi-2D smectics experimentally studied in DNA-cationic lipid complexes, [4,5]. In Sec. VII, we elucidate the extinction of hairpin dislocations. It goes on by annihilations of hairpin dislocations with polymer end points. In lyotropic smectics, rates of these processes are shown to be limited by a sluggish reptation of long semiflexible molecules, as well as by substantial energy barriers. We discuss the siginificance of these processes for understanding nonequilibrium phenomena in 2D smectics.

This paper is organized as follows: In Sec. II, we outline the physics of smectics and discuss the problem of wedge-shaped openings that are important for understanding voids accompanying hairpin dislocations in these materials. In Sec. III, we discuss the free energy of the turn that semiflexible polymer makes in the core of hairpin dislocations. In Sec. IV, we use the results of Secs. II and III to obtain our results for hairpin dislocations in both thermotropic and lyotropic 2D smectics. In Sec. V, we apply our results for lyotropic systems to entropically (sterically) stabilized systems of long semiflexible polymers. In Sec. VI, we discuss hairpin dislocations in smectics stabilized by electrostatic repulsion of the form appropriate for the smectics in DNA-cationic lipid complexes. In Sec. VII, we discuss the extinction of hairpin dislocations by annihilations with polymer end points. We summarize our results in Sec. VIII. Appendix A contains details relevant for the discussion in Sec. III. Appendix B discusses annihilation of two hairpins folded on a semiflexible polymer in a 2D smectic.

II. VOIDS IN 2D SMECTICS AND HAIRPIN TURNS

In this section, we briefly outline the physics of the smectic state and begin our discussion of hairpin turns in these materials. Free energy of a single hairpin dislocation involves two major distinct contributions

$$E_{\rm hp}=E_{\rm med}+E_{\rm turn}. \tag{2.1}$$

Here, $E_{\rm med}$ is the free-energy cost coming from the long-range smectic medium distortion being induced by the hairpin turn (see Fig. 1). Its presence introduces a void composed of two wedgelike openings in the smectic material, as depicted in Fig. 1. We discuss their energy in this section. The second term, $E_{\rm turn}$ in Eq. (2.1) is the energy localized in the turn that the semiflexible polymer makes at the very core

of the dislocation. It is discussed in the following section. Finally, in Sec. IV, we combine findings of Secs. II and III to obtain our results for hairpin dislocations in both thermotropic and lyotropic 2D smectics.

We start by considering a smectic stack of N long semiflexible molecules, each described by its height function above the x axis, $h_n(x)$, for the nth molecule. The thermodynamic potential of the stack at constant isotropic pressure P, is of the form

$$F_{sm}=P\int dx\,[h_N(x)-h_1(x)]+F_{\rm com}+F_{\rm bend}. \quad (2.2)$$

The first term in Eq. (2.2) is the standard pressure×system area term, whereas the term $F_{\rm com}$ is the compressional energy of the stack, of the form

$$F_{\rm com}=\sum_{n=1}^{N}\int dx\,V(h_{n+1}(x)-h_n(x)), \quad (2.3)$$

with $V[h_{n+1}(x)-h_n(x)]$ being the interaction potential between the neighboring semiflexible polymers (per their unit length). The last term in Eq. (2.2) is the bending energy of the stack, of the form

$$F_{\rm bend}=\sum_{n=1}^{N}\int dx\,\frac{\kappa}{2}\left(\frac{\partial^2 h_n(x)}{\partial x^2}\right)^2, \quad (2.4)$$

with κ is the single polymer bending constant. Here, and throughout this section, we discuss the smectic medium within the common ''paraxial approximation'' valid for small layer slopes, $dh_n/dx\ll 1$. We comment on this at the end of this section.

The smectic phase period $a=\langle h_{n+1}(x)-h_n(x)\rangle$ crucially depends on the competition between the first and the second term in Eq. (2.2). More suggestively, these two terms may be combined into one

$$F'_{\rm com}=\sum_{n=1}^{N}\int dx\,[V(h_{n+1}(x)-h_n(x)) + P[h_{n+1}(x)-h_n(x)]]. \quad (2.5)$$

Minimizing Eq. (2.5), with $h_{n+1}(x)-h_n(x)=a$, yields the smectic equation of state

$$P=-\frac{dV(a)}{da}, \quad (2.6)$$

for the equilibrium value of the smectic phase period a. For potentials $V(a)$ assuming absolute minimum for a particular value of a, Eq. (2.6) manifestly has a solution for a even for the zero value of the isotropic pressure P. Furthermore, applying here a sensible nonzero P typically produces only a small change of the smectic period a. Such a behavior is typical for *thermotropic* smectics. On the other side in typical *lyotropic* smectics, potentials $V(a)$ are dominantly repulsive, i.e., the right-hand side (RHS) of Eq. (2.6) is positive. Thus, $P>0$. In this case, the phase period a strongly depends on the applied value of the osmotic pressure P. Whatever is the case, by writing $h_n(x)=na+u(x,z)$, with $z=na$, and by expanding the above smectic free energy around its minimum, one obtains the usual 2D smectic elastic Hamiltonian [1],

$$H_{\rm el}=\int\int dx\,dz\left[\frac{B_{\rm sm}}{2}\left(\frac{\partial u}{\partial z}\right)^2+\frac{K_{\rm sm}}{2}\left(\frac{\partial^2 u}{\partial x^2}\right)^2\right], \quad (2.7)$$

with

$$B_{\rm sm}=-a\frac{dP(a)}{da}=a\frac{d^2V(a)}{da^2}, \quad (2.8)$$

the smectic compressibility modulus, and

$$K_{\rm sm}=\frac{\kappa}{a}, \quad (2.9)$$

the smectic bending modulus.

To discuss voids induced by a hairpin inserted between the nth and $n+1$st smectic layer (as in Fig. 1), we will need an effective free energy for these two layers, $F_{\rm eff}(h_n,h_{n+1})$. In general, $F_{\rm eff}$ is obtained by minimizing the system's free energy at fixed $h_n(x)$ and $h_{n+1}(x)$. By Eqs. (2.2) to (2.5), it must be of the form

$$F_{\rm eff}(h_n,h_{n+1})=\int dx\Bigg[V(h_{n+1}(x)-h_n(x)) + P[h_{n+1}(x)-h_n(x)]+\frac{\kappa}{2}\left(\frac{\partial^2 h_n(x)}{\partial x^2}\right)^2 + \frac{\kappa}{2}\left(\frac{\partial^2 h_{n+1}(x)}{\partial x^2}\right)^2\Bigg]+F_{\rm res}(h_n,h_{n+1}). \quad (2.10)$$

Here, the terms under the integral are the contributions of the nth and $n+1$st layer to the free-energy Eq. (2.2) [see Eqs. (2.4) and (2.5)]. The last term in Eq. (2.10), $F_{\rm res}$ is a residual contribution coming from minimizing the free-energy Eqs. (2.2)–(2.5) over configurations of layers that are either above the $n+1$st or below the nth layer. Physically, $F_{\rm res}$ arises due to *long-range* distortion of the smectic medium induced by the presence of dislocation voids in Fig. 1. Finding $F_{\rm res}$ thus reduces to a solved problem of finding the free energy of semi-infinite smectics above (or below) boundaries of given shapes [19], such as $h_n(x)$ and h_{n+1} here. We thus find,

$$F_{\rm res}(h_n,h_{n+1})=\int dx\,\frac{\delta\gamma}{2}\left[\left(\frac{\partial h_n(x)}{\partial x}\right)^2+\left(\frac{\partial h_{n+1}(x)}{\partial x}\right)^2\right], \quad (2.11)$$

with a ''surface tension''

$$\delta\gamma=B_{\rm sm}\lambda=\sqrt{B_{\rm sm}K_{\rm sm}}. \quad (2.12)$$

Here,

$$\lambda = \sqrt{\frac{K_{\rm sm}}{B_{\rm sm}}} \tag{2.13}$$

is the smectic penetration length [19]. The effective free energy in Eqs. (2.10) and (2.11) may be directly used to discuss shapes of symmetric wedges, such as those induced by the presence of a hairpin dislocation (Fig. 1). By writing

$$h_n = h_{\rm av} - z(x), \quad h_{n+1} = h_{\rm av} + z(x),$$

with $h_{\rm av}=(n+1/2)a$, and $2z(x)$, the wedge opening profile, one finds by Eqs. (2.10) and (2.11),

$$F_{\rm eff}(z) = \int dx \left[V(2z(x)) - V(a) + P[2z(x)-a] + \delta\gamma \left(\frac{dz}{dx}\right)^2 + \kappa \left(\frac{d^2z}{dx^2}\right)^2 \right]. \tag{2.14}$$

Here, for future convenience, we subtracted the free energy of the undistorted smectic configuration corresponding to $2z(x)=a$, with a determined by the Smectic equation of state (2.6). Effective free-energy Eq. (2.14) may be easily handled for profiles $z(x)$ that vary slowly over the length scale

$$L_b = \sqrt{\kappa/\delta\gamma} = \sqrt{a\lambda}, \tag{2.15}$$

at which the tension and the bending term in Eq. (2.14) balance. For such profiles, the bending term in Eq. (2.14) may be ignored. With this simplification (which is self-consistently justified in the following sections), the variation of the free-energy Eq. (2.14) yields the equation

$$\delta\gamma \frac{d^2z}{dx^2} = V'(2z) + P, \tag{2.16}$$

which is easily integrated once to yield

$$\delta\gamma \left(\frac{dz}{dx}\right)^2 - V[2z(x)] - 2z(x)P = -V(a) - aP, \tag{2.17}$$

that is,

$$\sqrt{\delta\gamma}\frac{dz}{dx} = \sqrt{V(2z) - V(a) + P(2z-a)}. \tag{2.18}$$

The integration constant on the RHS of Eq. (2.17) is chosen to correspond to a wedge profile with $2z(x)\to a$ as $x\to -\infty$. Equation (2.18) is easily combined with Eq. (2.14), to arrive at the following useful expression

$$F_w(D) = 2\int_{a/2}^{D/2} dz \sqrt{\delta\gamma[V(2z) - V(a) + P(2z-a)]}, \tag{2.19}$$

for the free energy of a wedge-shaped opening of the size D.

The presence of a hairpin dislocations in a smectic produces two such wedge-shaped voids, see Fig. 1. One is to the left and its opening size is actually $D+2a$, whereas the other one is to the right and its opening size is just D. The smectic medium energy contribution $E_{\rm med}$ in Eq. (2.1) can be thus estimated as,

$$E_{\rm med} = F_w(D+2a) + F_w(D). \tag{2.20}$$

To proceed, we discuss two typical cases of interest here. The first one are lyotropic materials with purely repulsive intermolecular potentials V, i.e., by Eq. (2.6), with generally positive osmotic pressure, $P>0$. For *large* wedge openings, $D \gg a$, the pressure terms dominates the integral in Eq. (2.19), yielding

$$F_w(D) \approx \frac{2}{3}\sqrt{P\delta\gamma}D^{3/2}. \tag{2.21}$$

In this limit, in the wedge-opening region, $a/2 \ll z(x) \ll D/2$, Eq. (2.16) reduces to $d^2z/dx^2 = P/\delta\gamma$. Thus, the wedge profile $z(x)$ is a nearly circular section with the radius

$$R = \frac{\delta\gamma}{P}, \tag{2.22}$$

as depicted in the Fig. 1(b). Furthermore, by $z(x)\approx x^2/2R$, one easily finds that the lateral size L of the voids in Fig. 1(b) is

$$L \approx \sqrt{RD} = \sqrt{\frac{D\delta\gamma}{P}}, \tag{2.23}$$

for $D \gg a$. We note that Eq. (2.22) has the form of the standard Laplace law $R=\sigma/\Delta p$, provided $\delta\gamma$ is identified as the interfacial tension σ, and the pressure difference $\Delta p = P - 0$, since the osmotic pressure inside a large void is $\approx$zero whereas outside of it is P.

The other case of interest here are thermotropic smectics stabilized by potentials V with a minimum at a preferred separation between molecules, with a repulsion at shorter distances and an attraction tail at longer distances. As noted before, such materials may be stable even at zero pressure P. Let us assume that the attraction has a short range comparable to a. Then, with $P=0$, for a large wedge-opening $D \gg a$, Eq. (2.19) yields,

$$F_w(D) \approx \sqrt{\delta\gamma|V(a)|}D. \tag{2.24}$$

In this limit, in the wedge-opening region, $a/2 \ll z(x) \ll D/2$, Eq. (2.16) reduces to $d^2z/dx^2 = 0$. Thus, the wedge profile $z(x)$ is a nearly straight line as depicted in Fig. 1(a). Its slope is, by Eq. (2.17) (with $x\to\infty$),

$$\tan(\theta) = \frac{dz}{dx} \approx \sqrt{\frac{|V(a)|}{\delta\gamma}}, \tag{2.25}$$

for smectics with interfacial tensions $\delta\gamma$ much larger than the smectic binding energy per unit length, $|V(a)|$. By Eq. (2.25), the lateral size L of the void in Fig. 1(a), is

$$L \approx \frac{D}{2\tan(\theta)} \approx \frac{D}{2}\sqrt{\frac{\delta\gamma}{|V(a)|}}. \tag{2.26}$$

Equation (2.25) may be phenomenologically interpreted in terms of a Young's law for contact angles, provided $\delta\gamma + |V(a)|/2$ is assumed to be the tension of the interfaces between the smectic medium and the voids in Fig. 1(a), and $2\delta\gamma$ is assumed to be the tension at a more subtle smectic-smectic ''interface'' away from the void region. By making such assumptions, de Gennes [14] obtains a contact angle essentially identical to that in Eq. (2.25) derived above from more microscopic considerations [20]. It is worthwhile noting that the problem discussed by de Gennes in [14], is that of lenticular smectic fractures of the critical size (the so-called Griffith size, [21,22]). Lenticular fractures are *unstable* void configurations (''critical nuclei'') that may appear only in the thermotropic case, corresponding to potentials $V(a)$ assuming a minimum at some finite a. Such solutions to our Eq. (2.16) [or Eq. (2.17)] actually appear only for *negative* pressures P tending to *open* the void. On the other hand, our main focus here is on the situations with $P>0$ (repulsive potentials) or $P=0$. In these cases, there are no lenticular fractures. Rather, the smectic medium surrounding the voids in Fig. 1 tends to close them. This tendency is counteracted by the bending elasticity of the turn that polymer makes in the dislocation core in Fig. 1. We discuss this highly curved polymer section separately, in the next section.

We conclude this section with a few important comments on the paraxial approximation employed in discussions of this section. It is exact for small wedge profile slopes, $dz/dx \ll 1$. It means, all of the above results are exact for hairpins with a small aspect ratio $D/2L \ll 1$ in Fig. 1. As discussed in the following sections, this is indeed the case if $\lambda \gg a$, with λ, the smectic penetration depth, Eq. (2.13). In Sec. IV, the same condition, $\lambda \gg a$, will be shown to ensure $D \gg a$ [so, Eqs. (2.21) to (2.25) are applicable], as well as $L \gg L_b$ [so bending energy terms in Eq. (2.14) could have been ignored, as was done above]. Thus, in 2D smectic materials with a relatively large $\lambda \gg a$, one has large hairpin turn dislocations with a large aspect ratio, $L \gg D \gg a$, as detailed in Sec. IV. Moreover, as shown in Sec. V, such large hairpin turns indeed occur throughout the entire stability range of entropically stabilized systems of long semiflexible polymers with purely hard-core repulsion [15,16]. Such systems are 2D analogs of fluid membrane phases stabilized by steric entropy [18]. We also discuss, in Sec. VI, hairpin turns in smectics stabilized by electrostatic repulsion of the form appropriate for the 2D smectics in DNA-cationic lipid complexes [4]. We find that such a repulsion may considerably depress the hairpin dislocation size and increase its energy.

III. ENERGY AND SHAPE OF POLYMER TURNS

In this section, we continue our discussion of hairpin turn dislocations by focusing now on the highly curved section that the semiflexible polymer makes in the core of the dislocation. We refer to it as the *turn* in the following. In Fig. 1, these turns appear like semicircular polymer sections between the contact points K. Their actual equilibrium shape is not a semicircle, as detailed in this section.

The number of monomers pulled out of the smectic medium (gray region in Fig. 1) into the turn section fluctuates in time. The polymer turn is thus an open subsystem exchanging its material with the grand-canonical bath constituted by the remaining polymer material, the smectic medium conceptualized as the gray region in Fig. 1. For turns of large sizes $D \gg a$, the interactions between the bath and the turn are significant only in a relatively small region near the two contact points K between them. In this case, all effects of the bath may be absorbed into a single thermodynamic variable μ, representing the chemical potential per unit length of the turn [23,24]. The shape of the turn may be thus obtained by varying grand-canonical free energy of the turn, of the form,

$$G_{\rm turn} = -\mu l + \int_0^l ds\, \frac{\kappa}{2} H^2. \tag{3.1}$$

Here, $l = \int ds$ is the arc length of the turn that can fluctuate at a fixed chemical potential μ, and $H = d\phi/ds$, the polymer curvature yielding its bending energy, the second term in Eq. (3.1); here, $\phi(s)$ is the local polymer slope angle with respect to a given axis [see Fig. 2]. In Eq. (3.1) and hereafter, we employ the standard arc-length s parametrization of the polymer shape. Grand-canonical free-energy Eq. (3.1) needs to be varied over all turn shapes and lengths l for fixed positions of the contacts K of the turn with the smectic medium. This yields equations determining the shape of the turn. We discuss them in Appendix A. These equations may be written in various interesting forms that are nontrivially related to each other [see Appendix A]. One of them is the second-order differential equation for the polymer curvature,

$$\mu \;\; H + \frac{\kappa}{2} H^3 + \kappa \frac{d^2 H}{ds^2} = 0, \tag{3.2}$$

which may be integrated once to yield

$$\frac{\mu}{2} H^2 + \frac{\kappa}{8} H^4 + \frac{\kappa}{2} \left(\frac{dH}{ds} \right)^2 = C_H, \tag{3.3}$$

with C_H an integration constant. As discussed in Appendix A, an alternative description of the polymer shape is by means of the sine-Gordon (''mathematical pendulum'') equation,

$$\kappa \frac{d^2 \phi}{ds^2} + \Lambda \sin[\phi(s) - \phi_0] = 0, \tag{3.4}$$

where Λ and ϕ_0 are constants. Equation (3.4) may be integrated once to yield

$$\frac{\kappa}{2} \left(\frac{d\phi}{ds} \right)^2 - \Lambda \cos[\phi(s) - \phi_0] = C_\phi, \tag{3.5}$$

where the ''pendulum energy'' C_ϕ is an integration constant.

There is a nontrivial relation between the above two alternative descriptions of the polymer shape. It is discussed in Appendix A. There we show that the description based on Eqs. (3.2) and (3.3) is equivalent to that in Eqs. (3.4) and (3.5), provided,

$$\Lambda^2 = \mu^2 + 2\kappa C_H, \quad C_\phi = -\mu, \tag{3.6}$$

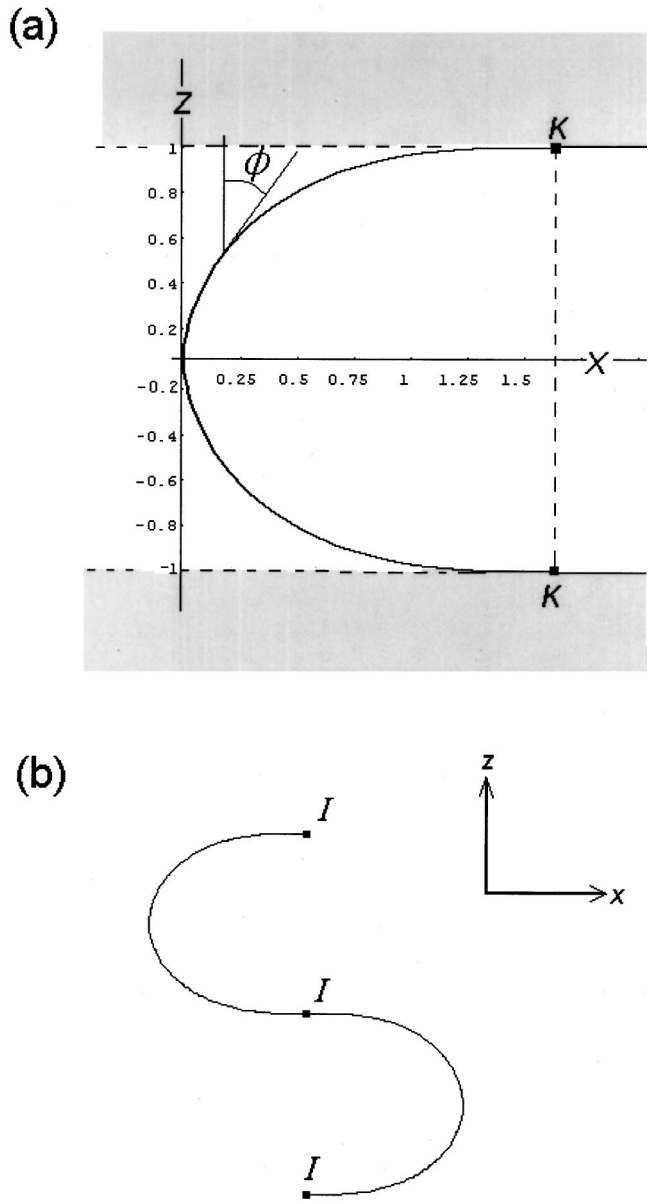

FIG. 2. (a) The universal polymer turn shape $[X(\phi),Z(\phi)]$. Here, ϕ is the polymer slope angle with respect to the z axis. At contact points K, with $\phi=\pm\pi/2$ and $[X_K,Z_K]=[2/C,\pm 1]$, the polymer curvature vanishes. Here, $X_K=2/C\approx 1.669\,24$. (b) One full period, S-shaped section of the *Elastica* curve, the half period of which is the C-shaped section in (a).

Each of the two descriptions has its own merits: The description in Eqs. (3.2) and (3.3) directly emerges from the original physical problem, i.e., the grand-canonical description Eq. (3.1) in which the turn length l may fluctuate at a constant chemical-potential μ. On the other hand, the sine-Gordon description in Eqs. (3.4) and (3.5) will more directly bring us to the final results for the turn shape and energy *provided* we relate the constants therein by using their relations in Eq. (3.6) to the parameters of the original physical problem (3.1) such as μ. It should be stressed that the emerging of the sine-Gordon description here is not surprising. It appears also in closely related Euler's *Elastica* problem of flexible rods bent in a plane under forces acting on their end points [25]. In the *Elastica* problem, the length of the rod l is held fixed (canonical ensemble-type problem). However, in the present problem, instead of having a rod of a fixed length, we have the turn, a polymer section with the length l that is not fixed. The number of monomers pulled out from the smectic medium into the turn section fluctuates and, thus, the arc-length l of the turn fluctuates also at a constant chemical-potential μ. Thus, here we have a grand-canonical ensemble-type problem.

To proceed, we need to know the appropriate value of the chemical potential per unit polymer length μ. It may be determined purely from the thermodynamic properties of the smectic bulk medium that plays here the role of the grand-canonical bath for the turn. μ may be related to the smectic phase period a by minimizing the grand-canonical free-energy density of the 2D smectic over a, [23,24]. Within a mean-field approach, grand-canonical smectic free-energy $G_{\rm sm}$ is simply obtained by considering a uniform smectic state with equidistant flexible polymers separated by a. One has $G_{\rm sm}=-\mu L_{\rm tot}+F_{\rm com}$; here, $F_{\rm com}$ is as in Eq. (2.3), and $L_{\rm tot}$ is the total length of all semiflexible polymers in the system. Assuming here equidistant polymers, the density $g_{\rm sm}$ of $G_{\rm sm}$ (per unit area) is easily shown to be

$$g_{\rm sm}=\frac{-\mu+V(a)}{a}. \tag{3.7}$$

Minimizing $g_{\rm sm}$ over a yields the equation,

$$\mu=-a\,\frac{dV(a)}{da}+V(a), \tag{3.8}$$

relating μ and a. We remark that, by Eqs. (3.7), (3.8), and (2.6), $g_{\rm sm}=dV/da=-P$, in accord with the standard relation between grand-canonical free-energy density and pressure [26]. To proceed, it will be useful to get a sense of the magnitude of μ in smectics. For lyotropic smectics with repulsive interactions $\{[dV(a)/da]=P>0\}$, one typically has $V(a)\sim -a[dV(a)/da]=aP(a)\sim a^2[d^2V(a)/da^2]=aB_{\rm sm}$, as illustrated in Secs. V and VI. Thus, by Eq. (3.8),

$$\mu\sim aB_{\rm sm}, \tag{3.9}$$

for typical lyotropic smectics. For them, by Eq. (3.8), μ is generally positive. On the other side, for thermotropic smectics in equilibrium at zero pressure $\{-[dV(a)/da]=P=0\}$, by Eq. (3.7), $\mu=V(a)=-|V(a)|<0$. Thus, μ is generally negative here, as the binding potential must be negative at its minimum $V(a)$. For usual potentials that depend on a single length scale$=a$, one has $-V(a)\sim a^2[\partial^2 V(a)/\partial a^2]=aB_{\rm sm}$. Thus,

$$|\mu|\sim aB_{\rm sm}, \tag{3.10}$$

for thermotropic smectics for zero (or small enough) pressure.

Equations (3.9) and (3.10) may be used to assess the relative significance of various terms in Eqs. (3.1)–(3.3) for the shape of the turn. As the curvature $H\sim 1/\textit{turn size}=1/D$, the

ratio between the chemical-potential terms and bending elasticity terms in Eqs. (3.1)–(3.3) behaves as $\mu/\kappa H^2 \sim \mu D^2/\kappa$, that is, by Eqs. (3.9), (3.10), (2.9), and (2.13), as

$$\frac{\mu}{\kappa H^2} \sim (D/\lambda)^2.$$

Thus, the chemical-potential terms may be ignored provided the turn size $D \ll \lambda$, the smectic penetration depth, Eq. (2.13). As detailed in Sec. IV, the condition $D \ll \lambda$ turns out to be satisfied for smectics with, actually, *large* turn sizes $D \gg a$ (e.g., over the entire stability range of the smectics stabilized by steric entropy, see Sec. V). Namely, in Sec. IV, we will find that for smectics with large turn size, $D \gg a$, the condition $D \ll \lambda$ is necessarily satisfied at the same time. Thus, for the materials with $a \ll \lambda$, one may set $\mu = 0$ in Eqs. (3.1)–(3.3). Thus, by Eq. (3.6), the turn shape problem reduces to solving Eq. (3.5) with $C_\phi = 0$,

$$\frac{\kappa}{2}\left(\frac{d\phi}{ds}\right)^2 = \Lambda \cos[\phi(s)]. \tag{3.11}$$

Here, we also set in Eq. (3.5), $\phi_0 = 0$, as appropriate in the coordinate system employed in the following (see Fig. 2). In the following, we will focus our attention on large turns $a \ll D \ll \lambda$ for which Eq. (3.11) is appropriate. Incidentally, only for such turns, with $D \gg a$, the separation of the hairpin dislocation energy into the medium and the turn contribution, Eq. (2.1) is exact, and the turn may be simply treated as a subsystem interacting with its grand-canonical bath only through the chemical-potential term, as assumed in Eq. (3.1). Otherwise, for the situations with $D \approx a \approx \lambda$, the interactions between the turn and its smectic bath need to be treated more precisely, making the hairpin dislocation problem difficult. We pursue a discussion of such a situation in Sec. VI. Here, we proceed with the discussion of turn shapes and energies as obtained from Eq. (3.11). We parametrize the points of the turn as $[x(s), z(s)]$, with $x(s)$ parallel, and $z(s)$ perpendicular to the equilibrium direction of smectic layers in Fig. 1 (see Fig. 2). Notably, $z(s)$ is in the range $-D/2 < z < +D/2$. The angle ϕ is convenient to measure with respect to the z axis, $\phi = \tan^{-1}(dx/dz)$, i.e., $dz/ds = \cos(\phi)$ and $dx/ds = \sin(\phi)$. By Eq. (3.11), we easily find the following useful relation for the bending energy of the turn,

$$E_{\rm turn} = \int ds \frac{\kappa}{2}\left(\frac{d\phi}{ds}\right)^2 = \Lambda \int ds \cos[\phi(s)]$$
$$= \Lambda \int_{-D/2}^{+D/2} dz = \Lambda \ D. \tag{3.12}$$

To find the constant Λ here, we transform the integral,

$$D = \int_{-D/2}^{+D/2} dz,$$

with $dz = ds\cos(\phi)$. Using here, by Eq. (3.11),

$$ds = d\phi \sqrt{\frac{\kappa}{2\Lambda \cos(\phi)}}, \tag{3.13}$$

we find

$$D = \sqrt{\frac{\kappa}{2\Lambda}} \int_{-\pi/2}^{+\pi/2} d\phi \sqrt{\cos(\phi)}. \tag{3.14}$$

Thus,

$$\Lambda = 2C^2 \frac{\kappa}{D^2}, \tag{3.15}$$

where C is an important numerical constant,

$$C = \tfrac{1}{2} \int_{-\pi/2}^{+\pi/2} d\phi \sqrt{\cos(\phi)} = \tfrac{1}{2} B(\tfrac{3}{4}, \tfrac{1}{2}) \approx 1.198\,14. \tag{3.16}$$

This constant plays a significant role in the results presented here and in the following sections. Equations (3.12) and (3.15) yield,

$$E_{\rm turn} = 2C^2 \frac{\kappa}{D} \approx 2.871\,07 \frac{\kappa}{D}, \tag{3.17}$$

for the bending energy of the polymer turn. By Eqs. (3.17) and (3.15), the contact force exerted by the turn on the surrounding smectic medium is

$$-\frac{dE_{\rm turn}}{dD} = 2C^2 \frac{\kappa}{D^2} = \Lambda. \tag{3.18}$$

In equilibrium, this force is balanced by the force exerted by the surrounding smectic medium on the turn, $dE_{\rm med}/dD$, with the medium energy $E_{\rm med}$ as in Eq. (2.20). This fact will be used in the following section to obtain equilibrium sizes and energies of hairpin-turn dislocations.

The form of the turn energy in Eq. (3.17) shows that the equilibrium shape of the turn is different from a semicircle that has $E_{\rm bend} = \pi\kappa/D$. This difference is further illustrated by looking at the actual shape of the turn, see Fig. 2(a). It is obtained by integrating the polymer shape equations $dz = \cos(\phi)ds$ and $dx = \sin(\phi)ds$. By Eqs. (3.13) and (3.15), these shape equations may be easily shown to yield the equations,

$$Z(\phi) = \frac{1}{C} \int_0^\phi d\phi' \sqrt{\cos(\phi')}, \tag{3.19a}$$

$$X(\phi) = \frac{1}{C} \int_0^\phi d\phi' \frac{\sin(\phi')}{\sqrt{\cos(\phi')}} = \frac{2(1-\sqrt{\cos(\phi)})}{C}, \tag{3.19b}$$

for the rescaled turn coordinates $Z = z/(D/2)$ and $X = x/(D/2)$. Equations (3.19a) and (3.19b), with ϕ in the range $(-\pi/2, +\pi/2)$ define an essentially universal turn shape, shown in Fig. 2(a). For $\phi \approx \pi/2$, we have a *contact point K* between the turn and the smectic medium (see the

following paragraph). By Eqs. (3.19a) and (3.19b) with $\phi=\pi/2$, the contact point is at $X_K=x_K/(D/2)=2/C\approx 1.669\,24$, and $Z_K=z_K/(D/2)=1$, as shown in Fig. 2(a). We note that Eqs. (3.19a) and (3.19b) can be used to derive the following alternative expression:

$$Z(X)=\pm\int_0^X dX'\frac{\left(1-\frac{1}{2}CX'\right)^2}{\sqrt{1-\left(1-\frac{1}{2}CX'\right)^4}},\quad 0<X<X_K=\frac{2}{C}, \tag{3.20}$$

for the universal shape of polymer turns depicted in Fig. 2(a). Mathematically, the *C*-shaped turn in Fig. 2(a) may be continued beyond the contact points. The continuation is a periodic *Elastica* curve shown in Fig. 2(b). Note that the *C*-shaped turn in Fig. 2(a) is one half of the full curve period in Fig. 2(b). Contact points *K*, with $\phi=\pm\pi/2$, in Fig. 2(a) actually correspond to the inflection points *I* in Fig. 2(b). These inflection points have a special feature: At them, *both* the slope $dz/dx=1/\tan(\phi)$ *and* the curvature $H=d\phi/ds$ vanish, in accord with our Eq. (3.11).

At the contact point *K*, the turn slope angle with respect to the *x* axis, $\theta=\pi/2-\phi$, is assumed above to be small, $\theta\ll 1$. Thus, $\phi\approx\pi/2$ at the contact point. This assumption is consistent with the use of Eq. (3.11) to obtain the turn shape and energy: As noted before in this section, this equation is appropriate for materials with $a\ll\lambda$. Furthermore, as discussed at the end of Sec. II and in Sec. IV, in materials with $a\ll\lambda$, profiles of wedge openings in Fig. 1 have small slope angles θ with respect to the *x* axis (''paraxial behavior''). Such wedge profiles touch the turn section at contact points with $\phi\approx\pi/2$. Moreover, as noted above, the turn curvature $H=d\phi/ds$ vanishes at contact points. This is consistent with a smooth matching of the polymer turn *C*-shaped section with the section of the *same* polymer that is to the right of its turn section in Fig. 1: The polymer section to the right of the turn is the interface between the right void and the smectic medium. Both the slope and curvature of this interface are small if $a\ll\lambda$, see Secs. II and IV. This interface smoothly matches with the turn profile at the contact point with $\phi\approx\pi/2$, at which both the turn slope $\theta=\pi/2-\phi$ and its curvature *H* are small.

Overall, for smectic materials with $a\ll\lambda$, one may combine the Sec. II paraxial approximation results for wedgelike void shapes and energies [Eqs. (2.21) and (2.24)] with the simple result for the turn energy Eq. (3.17) that corresponds to the universal turn shape in Fig. 2(a). This is used in the following section to obtain total energies of hairpin dislocations. These results are essentially *exact* in the limit of large $\lambda\gg a$. In the same limit, the polymer turn section approaches the universal shape depicted in Fig. 2(a), whereas the dislocation-induced voids depicted in Fig. 1 become highly anisotropic, with $a\ll D\ll L$, as detailed in the following section.

IV. HAIRPIN DISLOCATION SIZE AND ENERGY

In this section, we discuss hairpin dislocation size and energy by focusing on large hairpin turns with sizes *D* much bigger than the smectic phase period *a*. As anticipated in Secs. II and III, here, we show that such hairpin turns occur in smectic materials with $\lambda\gg a$, with λ, the smectic penetration length, Eq. (2.13). For these materials, by Eqs. (2.1), (2.20), and (3.17), hairpin dislocation energy is the sum of the energy of the two wedge-shaped openings and the turn bending energy, of the form,

$$E_{\rm hp}=2F_w(D)+2C^2\frac{\kappa}{D}, \tag{4.1}$$

for $D\gg a$. Equilibrium turn size and dislocation energy is simply obtained by minimizing Eq. (4.1) over *D*. In the following, we use this to discuss hairpin dislocations in typical lyotropic and thermotropic smectic materials introduced in Sec. II.

We first consider typical lyotropic smectic materials, with purely repulsive interactions between semiflexible polymers forming smectic layers. Such materials are in thermodynamic equilibrium only at positive values of the osmotic pressure *P*, see Sec. II. For $D\gg a$, the energy of wedge-shaped openings, $F_w(D)$, is here given by Eq. (2.21). With this, Eq. (4.1) reduces to

$$E_{\rm hp}=\tfrac{4}{3}\sqrt{P\delta\gamma}D^{3/2}+2C^2\frac{\kappa}{D}. \tag{4.2}$$

Minimizing Eq. (4.2) over *D* yields its equilibrium value

$$D_{\rm eq}=C^{4/5}\left(\frac{\kappa^2}{P\delta\gamma}\right)^{1/5}. \tag{4.3}$$

By Eqs. (2.23) and (4.3), the lateral size of the wedge-shaped voids in Fig. 1(b), is

$$L_{\rm eq}=C^{2/5}\left(\frac{\kappa(\delta\gamma)^2}{P^3}\right)^{1/5}. \tag{4.4}$$

By Eq. (4.2), the equilibrium dislocation energy is

$$E_{\rm hp}=\frac{10C^2}{3}\frac{\kappa}{D_{\rm eq}}=\frac{10C^{6/5}}{3}(\kappa^3P\delta\gamma)^{1/5}, \tag{4.5}$$

with $D_{\rm eq}$ as in Eq. (4.3). By Eqs. (4.2) and (4.5), the ratio between the medium contribution to $E_{\rm hp}$ [the first term in Eq. (4.2)] and the polymer turn contribution [the second term in Eq. (4.2)] is 2/3.

The dislocation length scales in Eqs. (4.2) to (4.4) may be expressed in terms of basic smectic length scales *a* and λ. To see this, we conveniently express the osmotic pressure *P* as

$$P=\Omega B_{\rm sm}. \tag{4.6}$$

Here, for typical lyotropic systems, the quantity Ω is typically a numerical constant of the order one, or, at most, a slowly changing function of the smectic period *a* [see the discussion above Eq. (3.9), and, also, the examples in Secs. V and VI]. By combining Eqs. (4.3), (4.4), and (4.6) with Eqs. (2.9), (2.12), and (2.13), we find

$$D_{\rm eq}=\frac{C^{4/5}}{\Omega^{1/5}}a^{2/5}\lambda^{3/5}, \tag{4.7}$$

and

$$L_{\rm eq}=\frac{C^{2/5}}{\Omega^{3/5}}a^{1/5}\lambda^{4/5}, \tag{4.8}$$

whereas the radius of the curvature of void interfaces [see Fig. 1(b) and Eq. (2.22)] is

$$R=\tfrac{1}{\Omega}\,\lambda. \tag{4.9}$$

Note that, by Eqs. (4.7) to (4.9),

$$D_{\rm eq}/a\sim(\lambda/a)^{3/5},\quad L_{\rm eq}/a\sim(\lambda/a)^{4/5},\quad R/a\sim(\lambda/a)^{1}. \tag{4.10}$$

Thus, in lyotropic 2D smectic materials with $\lambda\gg a$, one has a hierarchy of length scales related to hairpin-turn dislocations,

$$a\ll D_{\rm eq}\ll L_{\rm eq}\ll R\sim\lambda. \tag{4.11}$$

Equation (4.11) self-consistently confirms various assumptions beyond Eq. (4.2) we did in Secs. II and III, such as big turn size $D_{\rm eq}\gg a$, small aspect ratio $D_{\rm eq}/L_{\rm eq}\ll 1$ (paraxial approximation of Sec. II), and small $(D_{\rm eq}/\lambda)^2$ (needed to ignore the μ terms in Sec. III). All these conditions are self consistently satisfied in materials with small a/λ ratios. For example, by (4.10), the aspect ratio behaves as,

$$D_{\rm eq}/L_{\rm eq}\sim(a/\lambda)^{1/5}. \tag{4.12}$$

Also, by Eqs. (2.15) and (4.8), $L_b/L_{\rm eq}\sim(a/\lambda)^{3/10}\ll 1$, so the bending energy term in Eq. (2.14) could had been ignored as done in Sec. II. In the following section, we will see that the condition $\lambda\gg a$ is satisfied, for example, in lyotropic smectics stabilized by steric repulsion, yielding there large polymer turns with $D_{\rm eq}\gg a$ over essentially the entire stability range of these phases.

Another quantity of interest is the dislocation energy-temperature ratio, i.e., the quantity $E_{\rm hp}/2k_BT$ determining the average distance between hairpin-turn dislocations in thermodynamic equilibrium, see Eq. (1.1). By Eq. (4.5),

$$\frac{E_{\rm hp}}{2k_BT}=\frac{5C^2}{6}\,\frac{\xi_p}{D_{\rm eq}}=1.196\,28\,\frac{\xi_p}{D_{\rm eq}}. \tag{4.13}$$

Here,

$$\xi_p=\frac{2\kappa}{k_BT} \tag{4.14a}$$

is the semiflexible polymer persistence length, typically large at room temperature. By Eqs. (4.7) and (4.13),

$$\frac{E_{\rm hp}}{2k_BT}=\frac{5C^{6/5}\Omega^{1/5}}{6}\left(\frac{a}{\lambda}\right)^{3/5}\frac{\xi_p}{a}. \tag{4.14b}$$

We stress that energy-temperature ratio in Eq. (4.14b) is, for $a\ll\lambda$, substantially smaller than the simple estimate $E_{\rm hp}/k_BT\sim\xi_p/a$ one would obtain by naively assuming that the turn size $D_{\rm eq}\approx a$, see Sec. I, Eqs. (1.2), and (1.3). In fact, by Eqs. (4.13) and (1.3), we have

$$\frac{(E_{\rm hp})_{\rm naive}}{E_{\rm hp}}=\frac{3\pi}{10C^2}\,\frac{D_{\rm eq}}{a}=0.6565\,\frac{D_{\rm eq}}{a}, \tag{4.14c}$$

indicating that the naive theory in Eq. (1.2) substantially overestimates hairpin dislocation energy in the situations with $D_{\rm eq}\gg a$. In Secs. V and VI, we pursue further discussion of dislocation energies and sizes in various realistic lyotropic systems.

We now turn to the other type of smectic materials of interest that are thermotropic smectics stabilized by intermolecular potentials $V(a)$ with a minimum at a preferred separation between semiflexible molecules. As discussed in Sec. II, these smectics are stable even at zero pressure P. For these materials at $P=0$, the hairpin dislocation energy is, by Eqs. (4.1) and (2.24) given by

$$E_{\rm hp}=2\sqrt{\delta\gamma|V(a)|}D+2C^2\frac{\kappa}{D}, \tag{4.15}$$

for $D\gg a$. We recall that $|V(a)|$ is the binding energy (per unit length) for a pair of long semiflexible molecules. By minimizing Eq. (4.15) over a, we find,

$$D_{\rm eq}=C\sqrt{\frac{\kappa}{(\delta\gamma|V(a)|)^{1/2}}} \tag{4.16}$$

for the turn size. By Eqs. (2.26) and (4.16), the lateral size of the wedge-shaped voids in Fig. 1(a), is,

$$L_{\rm eq}=\frac{C}{2}\sqrt{\frac{\kappa(\delta\gamma)^{1/2}}{|V(a)|^{3/2}}}. \tag{4.17}$$

By Eqs. (4.15), the equilibrium hairpin dislocation energy here is

$$E_{\rm hp}=4C^2\frac{\kappa}{D_{\rm eq}}=4C\sqrt{\kappa(\delta\gamma|V(a)|)^{1/2}}, \tag{4.18}$$

with $D_{\rm eq}$ as in Eq. (4.16). By Eqs. (4.15) and (4.18), the smectic medium contribution to $E_{\rm hp}$ [the first term in Eq. (4.15)] is here equal to that of the polymer turn [the second term in Eq. (4.15)].

As for lyotropics, dislocation sizes for thermotropics, Eqs. (4.16) and (4.17), may be all expressed in terms of basic smectic length scales a and λ. However, forms of these dependencies are different for lyotropics and thermotropics. To see this, we express the value of the binding energy $|V(a)|$ per unit length as,

$$|V(a)|=\eta a B_{\rm sm}. \tag{4.19}$$

Here, $\eta=|V(a)|/[a^2V''(a)]$ is just a numerical constant dependent on the shape of the potential V [see the discussion above Eq. (3.10)]. By Eqs. (4.16), (4.17), and (4.19), combined with Eqs. (2.9), (2.12), and (2.13), we find

$$D_{\rm eq}=\frac{C}{\eta^{1/4}}a^{1/4}\lambda^{3/4} \tag{4.20}$$

and

$$L_{\rm eq}=\frac{D_{\rm eq}}{2\theta}=\frac{C}{2\eta^{3/4}}\frac{\lambda^{5/4}}{a^{1/4}}, \tag{4.21}$$

whereas the wedge slope angle θ [see Fig. 1(a) and Eq. (2.25)] is,

$$\theta=\eta^{1/4}\left(\frac{a}{\lambda}\right)^{1/2}. \tag{4.22}$$

Note that, by Eqs. (4.20) to (4.22),

$$D_{\rm eq}/a\sim(\lambda/a)^{3/4},\quad L_{\rm eq}/a\sim(\lambda/a)^{5/4}. \tag{4.23}$$

Thus, for thermotropic 2D smectics with $\lambda\gg a$, one has small wedge opening angles θ, and a hierarchy of length scales related to hairpin-turn dislocations,

$$a\ll D_{\rm eq}\ll\lambda\ll L_{\rm eq}. \tag{4.24}$$

Equation (4.24) self consistently confirms various assumptions beyond Eq. (4.15) we did before in Secs. II and III, such as big turn size $D_{\rm eq}\gg a$, small aspect ratio $D_{\rm eq}/L_{\rm eq}\sim\theta\ll 1$, and small $(D_{\rm eq}/\lambda)^2$. All these conditions are self consistently satisfied in thermotropic materials with small a/λ ratios. For example, by Eq. (4.23), the dislocation aspect ratio behaves here as,

$$D_{\rm eq}/L_{\rm eq}\sim(a/\lambda)^{1/2}. \tag{4.25}$$

Also, by Eqs. (2.15) and (4.21), $L_b/L_{\rm eq}\sim(a/\lambda)^{3/4}\ll 1$, so the bending energy term in Eq. (2.14) could had been ignored as was done in Sec. II.

Another quantity of interest for thermotropics is the dislocation energy-temperature ratio, i.e., the quantity $E_{\rm hp}/2k_BT$ determining the average distance between hairpin-turn dislocations in thermodynamic equilibrium, see Eq. (1.1). By Eq. (4.16),

$$\frac{E_{\rm hp}}{2k_BT}=C^2\frac{\xi_p}{D_{\rm eq}}. \tag{4.26a}$$

By Eqs. (4.20) and (4.26a),

$$\frac{E_{\rm hp}}{2k_BT}=C\,\eta^{1/4}\left(\frac{a}{\lambda}\right)^{3/4}\frac{\xi_p}{a}, \tag{4.26b}$$

We stress that energy-temperature ratio in Eq. (4.26a) is, for $a\ll\lambda$, substantially smaller than the simple estimate $E_{\rm hp}/k_BT\sim\xi_p/a$ one naively obtains by assuming that the turn size $D_{\rm eq}\approx a$, see Sec. I, Equations (1.2) and (1.3). In fact, by Eqs. (4.26a) and (1.3), we have

$$\frac{(E_{\rm hp})_{\rm naive}}{E_{\rm hp}}=\frac{\pi}{4C^2}\frac{D_{\rm eq}}{a}=0.5471\frac{D_{\rm eq}}{a}, \tag{4.26c}$$

indicating that the naive theory in Eq. (1.2) substantially overestimates hairpin dislocation energy in the situations with $D_{\rm eq}\gg a$.

To summarize this section, for thermotropic and lyotropic 2D smectics, we have derived simple expressions for hairpin dislocation sizes and energies. These quantities were related to basic materials properties, such as the smectic penetration length λ, the size of the smectic phase period a, and the semiflexible polymer persistence length ξ_p. Qualitative forms of these relations are found to be different for lyotropic and thermotropic smectic materials. Compare, for example, Eq. (4.10) with Eq. (4.23) for the dislocation sizes $D_{\rm eq}$ and $L_{\rm eq}$. Also, compare Eq. (4.14b) with Eq. (4.26b) for the dislocation energy-temperature ratio $E_D/2k_BT$. With this remark, we finish our general discussion of hairpin dislocation in various classes of 2D smectic materials. In the following sections, we apply our results to hairpin dislocations in several interesting examples of lyotropic 2D smectics. We note that the anomalous elasticity effects present at long length scales in 2D smectics [2], may be ignored in the present discussions: The lateral size of hairpins $L_{\rm eq}$ turns out to be much smaller than the anomalous Ginzburg length scale $\xi_{\rm Gx}=8\pi K_{\rm sm}^{3/2}/k_BTB_{\rm sm}=4\pi\xi_p\lambda/a$. For example, for lyotropics, by Eq. (4.7), $L_{\rm eq}/\xi_{\rm Gx}=(\Omega^{3/5}/4\pi C^{2/5})(a/\xi_p)(a/\lambda)^{1/5}<1$ in all of the situations discussed here and in the following sections. Likewise, we ignored the softening of the polymer bending stiffness κ due to thermal fluctuations (see, e.g., Ref. [11]). This effect is potentially strong along the polymer turn section, which is nearly free. It would reduce κ by an amount $|\delta\kappa|\sim k_BT\,D_{\rm eq}$. However, the relative change of the stiffness constant, $|\delta\kappa|/\kappa\sim D_{\rm eq}/\xi_p$ is small as, generally, $D_{\rm eq}\ll\xi_p$. An exception is sterically stabilized phases in the vicinity of their transition to isotropic liquid phase, where $D\approx a\approx\xi_p$, see the following section. However, as $D_{\rm eq}/\xi_p\sim(a/\xi_p)^{3/5}$ [see Eq. (5.7) below], the softening of κ is quantitatively insignificant for the interesting effects in sterically stabilized phases discussed in Sec. V. An example is a sharp maximum of the D/a ratio that we find at an a much smaller than ξ_p [see Fig. 3(a), and Eqs. (5.12) and (5.13) below]. This effect, rather than the thermal softening of the bending stiffness constant, produces a significant reduction of the hairpin dislocation energy in respect to that obtained from the naive hairpin picture [see Eqs. (1.2), (1.3), and (4.14c), and the discussions in following section].

V. HAIRPIN DISLOCATIONS IN STERICALLY STABILIZED 2D SMECTICS

Here, and in the following section, we apply our results to two interesting classes of lyotropic stabilized by repulsive interactions between long semiflexible polymers. In this section, we discuss hairpin-turn dislocations in 2D smectics with purely hard-core repulsion interaction between neighboring polymers [15,16]. Such phases are 2D analogs of extensively studied 3D lamellar phases of membranes repelling each other with a short-range repulsion [18,9–11]. Similar to the membrane phases, in the absence of long-range repulsion, interactions between long molecules are dominated by

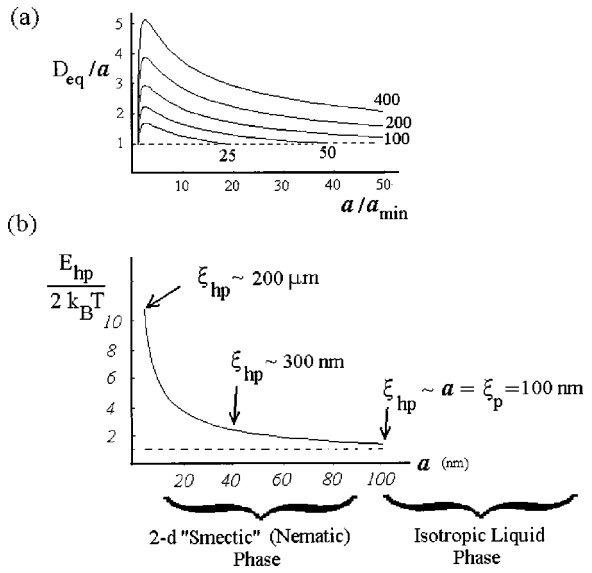

FIG. 3. (a) The ratio D_{eq}/a versus a/a_{min} for sterically stabilized 2D smectic phases of long semiflexible molecules. The ratio is plotted for several values of the persistence length-to-diameter ratio, $\xi_p/a_{min}=25$, 50, 100, 200, 400. In all cases, D_{eq}/a reaches its maximum for $a/a_{min}=5/2$: $(D_{eq}/a)_{max}=0.4655(\xi_p/a_{min})^{2/5}$ [see Eqs. (5.12) and (5.13)]. We remark that, likewise to D_{eq}/a, the ratios L_{eq}/a and R_{eq}/a reach their maximum for $a/a_{min}=15/8$ and 3/2, respectively. By Eqs. (5.8) and (5.9), these maximum values are found to be: $(L_{eq}/a)_{max}=0.4661\ (\xi_p/a_{min})^{8/15}$ and $(R_{eq}/a)_{max}=0.5016\ (\xi_p/a_{min})^{2/3}$. (b) The hairpin dislocation energy-to-temperature ratio $E_{hp}/2k_BT$ versus smectic phase period a, for a sterically stabilized phase of semiflexible molecules with the persistence length $\xi_p=100$ nm and molecular diameter $a_{min}=2$ nm. Note that the separation between hairpin dislocations ξ_{hp} rapidly decreases with increasing a. For $a\to\xi_p$, $E_{hp}/2k_BT\sim 1$, and the hairpin separation ξ_{hp} drops to a value $\approx a\approx\xi_p$. There, the hairpin ensemble becomes dense, and the 2D smectic (in fact, a nematic) melts into an isotropic liquid phase.

entropic effects (steric entropy), [15–17]. They yield an effective long-range potential of the form

$$V(a)=A\frac{k_BT}{(\xi_p/2)^{1/3}(a-a_{min})^{2/3}}. \tag{5.1}$$

Here, a_{min} is the cross-section diameter of molecules representing the smallest possible value of the smectic phase period. a_{min} is typically much smaller than the polymer persistence length ξ_p, Equation (4.14a), which also enters Eq. (5.1). The quantity A in Eq. (5.1) is a numerical constant. It may be estimated from a simple polymer-in-a-tube-model, yielding [17]

$$A\approx 1.1036. \tag{5.2}$$

By Eqs. (5.1), (2.6), and (2.8), the osmotic pressure and the smectic compressibility are here given by

$$P=\frac{2A}{3}\frac{k_BT}{(\xi_p/2)^{1/3}(a-a_{min})^{5/3}} \tag{5.3}$$

and

$$B_{sm}=\frac{10A}{9}\frac{k_BTa}{(\xi_p/2)^{1/3}(a-a_{min})^{8/3}}. \tag{5.4}$$

Thus, by Eq. (4.6),

$$\Omega=\frac{P}{B_{sm}}=\frac{3}{5}\left(1-\frac{a_{min}}{a}\right). \tag{5.5}$$

The smectic penetration length Eq. (2.13) is, by Eqs. (5.4), (2.9), and (4.14),

$$\lambda=\frac{3}{\sqrt{10A}}(\xi_p/2)^{2/3}a^{1/3}\left(1-\frac{a_{min}}{a}\right)^{4/3}$$
$$=0.9030(\xi_p/2)^{2/3}a^{1/3}\left(1-\frac{a_{min}}{a}\right)^{4/3}. \tag{5.6}$$

Equations (5.3)–(5.6) may be combined with Eqs. (4.7)–(4.9) to find the equilibrium hairpin dislocation sizes in Fig. 1(b):

$$D_{eq}=C^{4/5}\left(\frac{5}{3}\right)^{1/5}\left(\frac{3}{\sqrt{10A}}\right)^{3/5}(\xi_p/2)^{2/5}(a-a_{min})^{3/5}$$
$$=1.2039(\xi_p/2)^{2/5}(a-a_{min})^{3/5}, \tag{5.7}$$

$$L_{eq}=C^{2/5}\left(\frac{5}{3}\right)^{3/5}\left(\frac{3}{\sqrt{10A}}\right)^{4/5}(\xi_p/2)^{8/15}(a-a_{min})^{7/15}$$
$$=1.3461(\xi_p/2)^{8/15}(a-a_{min})^{7/15}, \tag{5.8}$$

and

$$R_{eq}=53\frac{3}{\sqrt{10A}}(\xi_p/2)^{2/3}(a-a_{min})^{1/3}$$
$$=1.5050(\xi_p/2)^{2/3}(a-a_{min})^{1/3}. \tag{5.9}$$

The hairpin dislocation energy-temperature ratio Eq. (4.13) is here

$$\frac{E_{hp}}{2k_BT}=C^{6/5}\left(\frac{5}{3}\right)^{4/5}\left(\frac{\sqrt{10A}}{3}\right)^{3/5}\left(\frac{\xi_p/2}{a-a_{min}}\right)^{3/5}$$
$$=1.9873\left(\frac{\xi_p/2}{a-a_{min}}\right)^{3/5}. \tag{5.10}$$

Results in Eqs. (5.7)–(5.10) are applicable in the range of smectic periods a for which Eq. (5.7) yields $D_{eq}>a$. By Eq. (5.7), we find

$$\frac{D_{eq}}{a}=C^{4/5}\left(\frac{5}{3}\right)^{1/5}\left(\frac{3}{\sqrt{10A}}\right)^{3/5}\left(\frac{\xi_p/2}{a}\right)^{2/5}\left(1-\frac{a_{min}}{a}\right)^{3/5}$$
$$=1.2039\left(\frac{\xi_p/2}{a}\right)^{2/5}\left(1-\frac{a_{min}}{a}\right)^{3/5}, \tag{5.11}$$

valid in the range of a in which $D_{\rm eq}/a>1$. In Fig. 3(a), we plot the $D_{\rm eq}/a$ ratio versus $a/a_{\rm min}$, for several different values of the ratio $\xi_p/a_{\rm min}$. We see that this ratio as a function of a has a maximum. By Eq. (5.11), the $D_{\rm eq}/a$ ratio reaches its maximum value

$$\left(\frac{D_{\rm eq}}{a}\right)_{\rm max}=C^{4/5}\left(\frac{3}{25}\right)^{2/5}\left(\frac{3}{\sqrt{10A}}\right)^{3/5}\left(\frac{\xi_p}{a_{\rm min}}\right)^{2/5}=0.4655\left(\frac{\xi_p}{a_{\rm min}}\right)^{2/5}, \tag{5.12}$$

when the smectic period a reaches the characteristic value a_0 given by

$$a_0=\tfrac{5}{2}\,a_{\rm min}. \tag{5.13}$$

By Eq. (5.12), the maximum value the ratio $D_{\rm eq}/a$ may attain is limited purely by a finite value of the polymer diameter $a_{\rm min}$. For infinitely thin polymer lines, the quantity $(D_{\rm eq}/a)_{\rm max}$ would diverge. By Eq. (5.12), this maximum is controlled by the ratio $\xi_p/a_{\rm min}$, which is big for realistic semiflexible polymers. Thus, by Eqs. (5.11) and (5.12), the equilibrium size of hairpin turns $D_{\rm eq}$ is *a priori* much bigger than the period a of sterically stabilized phases of long molecules, as documented in Fig. 3(a). In fact, by Eq. (5.11), $D_{\rm eq}>a$ over essentially the entire stability range of these phases. The ratio $D_{\rm eq}/a$ approaches one in only two characteristic limits: One of them corresponds to a highly swollen phase with the period a given by

$$a_{\rm max}=\frac{C^2}{2}\left(\frac{5}{3}\right)^{1/2}\left(\frac{3}{\sqrt{10A}}\right)^{3/2}\xi_p=0.7952\xi_p. \tag{5.14}$$

Such a state, with the period a comparable to the polymer persistence length ξ_p, is at the border line for the phase transition to a more disordered, isotropic liquid state of polymers (much like what happens in 3D fluid membrane phases, [27–29,23,24]). Note that this is actually the nematic-to-isotropic phase transition (recall that, as noted in Sec. I, dislocations are free and turn 2D smectics into nematics [1]). Close to this transition, by Eq. (5.10) with $a\approx\xi_p$, the hairpin dislocation free-energy $E_{\rm hp}\approx k_BT$ [see Fig. 3(b)], and thus the dislocation ensemble becomes dense [see Eq. (1.1)], signaling an onset of a nearby isotropic phase. In the vicinity of this transition, the turn size $D_{\rm eq}\approx a\approx\lambda\approx\xi_p$. Moving away from the transition, by decreasing the phase period a, initially causes an increase of the $D_{\rm eq}/a$ ratio up to its maximum value $(D_{\rm eq}/a)_{\rm max}\sim(\xi_p/a_{\rm min})^{2/5}\gg 1$, Eq. (5.12), occurring for $a=5a_{\rm min}/2$ [see Fig. 3(a)]. A further decrease of a causes a decrease of the $D_{\rm eq}/a$ ratio until it, once again, becomes one [see Fig. 3(a)]. By Eq. (5.11), this happens at relatively small periods, $a\sim a'_{\rm min}$, with $a'_{\rm min}$ given by

$$\frac{a'_{\rm min}-a_{\rm min}}{a'_{\rm min}}=C^{-4/3}\left(\frac{3}{5}\right)^{1/3}\frac{\sqrt{10A}}{3}\left(\frac{a_{\rm min}}{\xi_p/2}\right)^{2/3}=0.7339\left(\frac{a_{\rm min}}{\xi_p/2}\right)^{2/3}. \tag{5.15}$$

By Eq. (5.15), for realistic semiflexible molecules with $\xi_p\gg a_{\rm min}$, $a'_{\rm min}-a_{\rm min}$ is only a relatively small fraction of the molecular diameter $a_{\rm min}$.

Thus, through essentially the entire range of entropically stabilized smectic phases of long semiflexible molecules, hairpin dislocations have turn sizes $D_{\rm eq}$ significantly bigger than the phase period a. Moreover, interestingly, the ratio $D_{\rm eq}/a$ reaches its maximum value $(D_{\rm eq}/a)_{\rm max}\sim(\xi_p/a_{\rm min})^{2/5}\gg 1$, Eq. (5.12), for a characteristic value of the phase period, $a_0=5a_{\rm min}/2$. Figure 3(a) gives the ratio $D_{\rm eq}/a$ versus $a/a_{\rm min}$ for several different values of $\xi_p/a_{\rm min}$. For a quantitative illustration, let us consider semiflexible polymers with $\xi_p=100\,$nm and $a_{\rm min}=2\,$nm, with a moderate ratio $\xi_p/a_{\rm min}=50$. For ensembles of these molecules, with only short-range repulsion, a sterically stabilized smectic state occurs for intermolecular separations a in the range $a_{\rm min}=2\,{\rm nm}<a<a_{\rm max}\sim\xi_p=100\,{\rm nm}$. By Eqs. (5.12) and (5.15), the ratio $D_{\rm eq}/a$ reaches its maximum value $(D_{\rm eq}/a)_{\rm max}\approx 2.2$, for the polymer separation $a=a_0=5\,$nm. For this particular separation, the polymer turn size $D_{\rm eq}\approx 11\,$nm, whereas the size of the wedge-shaped voids accompanying the dislocation [see Fig. 1(b)] is, by Eq. (5.8), $L_{\rm eq}\approx 18\,$nm. The radius of the curvature of wedges [see Fig. 1(b)] is, by Eq. (5.9), $R_{\rm eq}\approx 30\,$nm. These numbers illustrate the hierarchy of dislocation length scales emphasized before in Eq. (4.11):

$$a=5\ {\rm nm}<D_{\rm eq}=11\ {\rm nm}<L_{\rm eq}=18\ {\rm nm}<R_{\rm eq}=30\ {\rm nm}, \tag{5.16}$$

for molecules with $\xi_p=100\,$nm and $a_{\rm min}=2\,$nm. Such ordering of hairpin dislocation length scales, $a<D_{\rm eq}<L_{\rm eq}<R_{\rm eq}$, emphasized before in Sec. IV [see Eq. (4.11)] occurs throughout the entire stability range of sterically stabilized phases. In fact, by Eqs. (5.7)–(5.8), $a\approx D_{\rm eq}\approx L_{\rm eq}\approx R_{\rm eq}$ only in the limits $a\to a_{\rm max}\sim\xi_p$ and $a\to a'_{\rm min}\approx a_{\rm min}$.

The dislocation energy-temperature ratio in Eq. (5.10) is of the order one only close to the border line with the isotropic liquid phase at $a\sim\xi_p$, see Fig. 3(b). Moving away from this border line increases the $E_{\rm hp}/2k_BT$ ratio, and, by Eq. (1.1), increases the average separation between hairpin dislocations $\xi_{\rm hp}$. Thus, for semiflexible molecules with $\xi_p=100\,$nm, and $a_{\rm min}=2\,$nm, we estimate $\xi_{\rm hp}\sim 300\,$nm for $a=40\,$nm, $\xi_{\rm hp}\sim 700\,$nm for $a=20\,$nm, while $\xi_{\rm hp}\sim 200\,\mu$m for $a=5\,$nm corresponding to the example in Eq. (5.16) for which $E_{\rm hp}/2k_BT=10.7$ and $D_{\rm eq}/a=2.2$. We note that the naive hairpin dislocation theory in Eqs. (1.2) and (1.3) yields $\xi_{\rm hp}\sim 3\,$cm for the last example with $a=5\,$nm. This more than ten times larger $\xi_{\rm hp}$ is predicted by the simple theory because it ignores the possibility of hairpin core expansion into the surrounding smectic medium to a size $D_{\rm eq}$ bigger than the phase period a. Going with this expansion is a considerable reduction of the hairpin dislocation energy, see Eq. (4.14c). Because of the exponential dependence of $\xi_{\rm hp}$ on the hairpin energy, this effect is significant even in the situations when a relatively small $D_{\rm eq}/a$ ratio occurs, as illustrated by the above example. This core expansion effect is strongest for the phase separation $a=2.5a_{\rm min}$ at which the $D_{\rm eq}/a$ ratio is maximal, see Eqs. (4.14c), (5.12), and (5.13): For this phase period, $(E_{\rm hp})_{\rm naive}/E_{\rm hp}\sim(\xi_p/a_{\rm min})^{2/5}$, and the naive

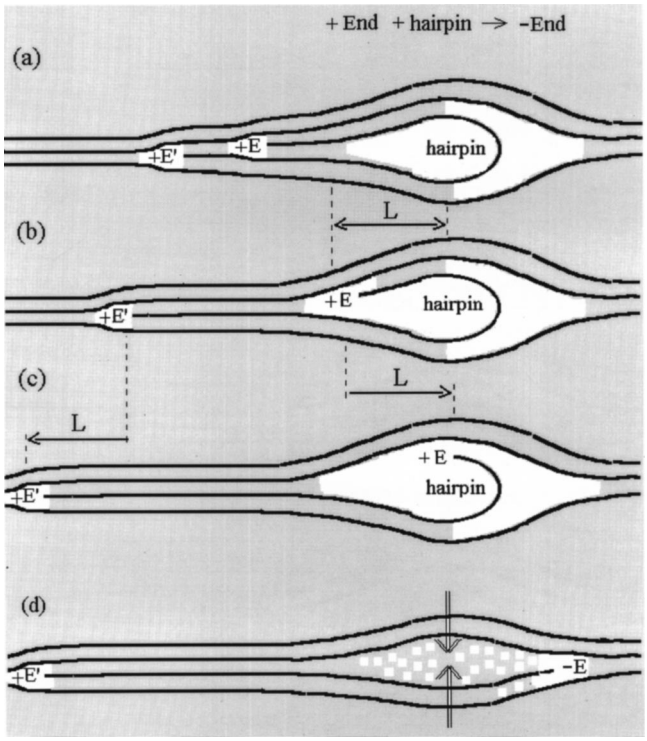

FIG. 4. Annihilation of a hairpin turn dislocation by a polymer end-point dislocation. Result is an end-point dislocation $-E$ in (d), with topological charge opposite to that of the original end-point dislocation $+E$ in (a). An energy barrier needs to be overcome in order for the end point $+E$ to move from a metastable state in (b) to an unstable transition state in (c) preceding the annihilation moment (see text). Subsequently, the polymer end flips and produces the $-E$ end-point dislocation, whereas the void formerly occupied by the hairpin closes, as depicted in (d). Note that the motion of the polymer end points $+E$ and $+E'$ is mediated by polymer reptation leaving the position of the hairpin intact.

theory substantially overestimates hairpin dislocation energies in sterically stabilized 2D smectic phases of very stiff polymers.

For small phase periods, $a \ll \xi_p$, hairpin dislocations have substantial energies and must be rare in systems that are in true thermodynamic equilibrium, see Eq. (5.10) and Fig. 3(b). However, as detailed in Sec. VII, such systems, characterized by a low-equilibrium dislocation concentration, coincidentally have long-time scales needed to reach the true thermodynamic equilibrium. In Sec. VII, we find that such systems may maintain relatively large *nonequilibrium* densities of hairpin dislocations possibly present in the early stage of the smectic phase ordering from a more disordered state (e.g., isotropic polymer liquid). Lyotropics with large $E_{\rm hp}$ coincidentally exhibit large energy barriers for the processes of hairpin annihilations with polymer end points that extinguish these dislocations (see Fig. 4). Moreover, the dynamics of this process is mediated by a sluggish reptation of long semiflexible molecules, as detailed in Sec. VII. In such materials, large initial nonequilibrium hairpin dislocation densities decay slowly and true thermodynamic equilibrium may be hard to reach on realistic time scales.

VI. HAIRPIN DISLOCATIONS IN DNA-CATIONIC LIPID COMPLEXES

In this section, we discuss hairpin dislocations in complexes of long DNA molecules mixed with cationic lipid molecules. These complexes have been the subject of a number of recent experimental and theoretical studies [3–8]. Under some circumstances, these complexes form a 3D lamellar membrane phase with DNA molecules intercalated in galleries between lipid membranes [3,4]. Interactions between DNA molecules in different galleries are experimentally evidenced to be weak. Thus, to a good approximation, we may consider these so-called sliding phases [6–8] as stacks of weakly interacting 2D smectics in which DNA molecules play the role of smectic layers. These phases are stabilized by complex repulsive interactions of electrostatic origin [3,4]. Their detailed form is not well known. To discuss hairpin dislocations in these phases, we consider the following semiempirical form for the osmotic pressure between DNA molecules:

$$P(a) = C_e \frac{k_B T}{l_B (a - a_{\rm es})}, \quad C_e \approx 7.2 \pm 0.6, \tag{6.1}$$

suggested by Salditt *et al.*, Ref. [4]. Here, l_B is the so-called Bjerrum length; $l_B \approx 0.7$ nm in water at room temperature. $a_{\rm es}$ in Eq. (6.1) is an electrostatic diameter of DNA; $a_{\rm es} \approx 0.4$ nm at most, some five times smaller than the actual diameter of DNA, $a_{\rm min} \approx 2$ nm. By Eqs. (6.1) and (2.8), the smectic compressibility modulus is given here by

$$B_{\rm sm} = C_e \frac{k_B T a}{l_B (a - a_{\rm es})^2}. \tag{6.2}$$

The quantity Ω in Eq. (4.6) here assumes the simple form

$$\Omega = \frac{P}{B_{\rm sm}} = 1 - \frac{a_{\rm es}}{a}. \tag{6.3}$$

As $a > a_{\rm min} \approx 5 a_{\rm es}$, Ω is approximately one in practical situations. The smectic penetration length Eq. (2.13) is, by Eqs. (6.2), (2.9), and (4.14), given here by

$$\lambda(a) = \lambda_0 \left(1 - \frac{a_{\rm es}}{a} \right), \tag{6.4}$$

with

$$\lambda_0 = \sqrt{\frac{\xi_p l_B}{2 C_e}}. \tag{6.5}$$

As $a > a_{\rm min} \approx 5 a_{\rm es}$, to a good approximation $\lambda(a) \approx \lambda_0$ and $\Omega \approx 1$. Notably, λ here does not significantly depend on the phase period a, in marked contrast to the penetration depth in entropically stabilized phases [see Eq. (5.6)]. With $l_B = 0.7$ nm, for DNA with typical values of $\xi_p = 50$–100 nm, by Eq. (6.5), the penetration length is in the range $\lambda = 1.5$–2.1 nm. Hairpin dislocation size and energy here may be now estimated by using the results of Sec. IV. In the experiments [3,4], the phase period a is continuously varied

in a range above 2.5 nm. In this range, the above estimate for λ is comparable to a. Thus, the estimates of Sec. IV may be used to gain a sound qualitative insight only. For example, by Eq. (4.7) with $a=2.5$ nm and with $\lambda=2.1$ nm, one finds $D_{\rm eq}=2.6$ nm. Thus, in the experimentally achieved situations, the turn size $D_{\rm eq}$ is essentially the same as the phase period. Furthermore, for example, by Eq. (4.13) with $D_{\rm eq}\approx a=2.5$ nm and $\xi_p=50$ nm, the dislocation energy-temperature ratio $E_{\rm hp}/2k_BT\approx 24$. Thus, by Eq. (1.1), the equilibrium distance between hairpin dislocations is some $\exp(E_{\rm hp}/2k_BT)\sim 10^{10}$ times larger than the phase period a. The interlayer couplings ignored here may only increase this distance [6–8].

These estimates support the conjecture of previous studies [8], that hairpin dislocations are rare in these systems in thermodynamic equilibrium. It should be stressed though that the actual experimental DNA-cationic lipid systems may easily have much larger *nonequilibrium* concentration of defects such as hairpin dislocations created in the early stage of the phase formation. Such nonequilibrium hairpin dislocation concentrations may decay very slowly to its equilibrium value. This decay involves sluggish annihilations of hairpins by semiflexible polymer end points, see Sec. VII. On realistic experimental time scales, DNA-cationic lipid complexes may easily exhibit a substantional nonequilibrium concentration of hairpin dislocations.

VII. ANNIHILATIONS OF HAIRPIN DISLOCATIONS

A potentially more important type of dislocations in DNA-cationic complexes are polymer end points. They may be envisioned as wedge-shaped voids in the smectic medium, with the vertical size $\approx 2a$, see Fig. 4. As detailed elsewhere [30], the ideas of Sec. II may be used to calculate the end-point dislocation energy $E_{\rm ep}$. It is only few k_BT large for DNA-cationic lipid complexes systems discussed in Sec. VI. In practice, one deals with systems with a huge length l of semiflexible molecules, such as λ-DNA used in these complexes, with $l=16\,000$ nm$\gg a\sim 3$ nm, [4]. In such systems, the attractions between end-point dislocations with opposite topological charge are week compared to end-point positional entropy effects [30]. There, almost all end points are free dislocations and the density of free end-point dislocations $n_{\rm ep}=1/la$. (Note that each polymer, occupying area $=la$, contributes two end-point dislocations: the left end point with the topological charge $T=+1$, and the right end point with topological charge $T=-1$.) Thus, the smectic coherence length scale (above which it behaves as a nematic) may be simply estimated as

$$\xi_{\rm ep}=\frac{1}{\sqrt{n_{\rm ep}}}=\sqrt{la}, \tag{7.1}$$

yielding, for example, $\xi_{\rm ep}=200$ nm for $l=16\,000$ nm and $a=2.5$ nm. This length scale sets the minimum size of monodomains needed to clearly see the nematic behavior in the experiments on λ-DNA-cationic lipid complexes [31].

As the equilibrium concentration of hairpins is much smaller than that of polymer end points, typical faith of a hairpin introduced (in a *nonequilibrium* situation) is to be extinct. Away from sample boundaries, the most rapid processes for this extinction are annihilations of hairpins with end-point dislocations. This is illustrated in Fig. 4, depicting the process

$$\text{plus-end-point} + \text{hairpin} \rightarrow \text{minus-end-point}, \tag{7.2}$$

which preserves the total topological charge: the end point $+E$ with $T=+1$ approaches the hairpin with $T=-2$ [Fig. 4(a)–4(c)], to annihilate it and produce $-E$ end point with $T=-1$, as depicted in Fig. 4(d), showing also the relaxation of the void formerly occupied by the hairpin. The motion of the end points $+E$ and $+E'$ in Fig. 4 is mediated by reptation of the semiflexible polymer along its contour length. This diffusive collective motion of the whole polymer leaves the hairpin position in space intact (see Fig. 4). The polymer reptation is capable to bring one of the two end points into the hairpin void region (white areas in Fig. 4). Thus, say $+E$, will eventually enter the void to form a composite with the hairpin dislocation, depicted in Fig. 4(b) (with total topological charge$=-1$). The state in Fig. 4(b) is actually metastable: moving away from it, either back to the state in Fig. 4(a) or to that in Fig. 4(c) costs energy. Indeed, moving E to the left, back to the smectic medium, recreates the original end-point dislocation and causes an energy cost $\approx E_{\rm ep}$. On the other hand, moving E in Fig. 4(b) to the right by the displacement$=L$, causes an equal in magnitude displacement of the *other* end-point E' deeper into the smectic medium [see Figs. 4(b) and 4(c)]. This displacement goes on with an energy cost due to a work W_L needed to be done against the osmotic pressure force$=Pa$ acting on the imbedded end point E':

$$W_L=PaL. \tag{7.3}$$

By Eq. (7.3) and our results for hairpins in lyotropics [see Eqs. (4.3) to (4.5)],

$$W_L=\frac{3}{10}\frac{a}{D_{\rm eq}}E_{\rm hp}, \tag{7.4}$$

for lyotropics with $D_{\rm eq}\gg a$. Thus, W_L is smaller than $E_{\rm hp}$ by the factor $\sim a/D$. On the other hand, W_L is expected to be bigger than the energy of end-point dislocations $E_{\rm ep}$ in lyotropics: For them we have, by Eq. (2.21),

$$E_{\rm ep}\sim F_w(D=2a)\sim\left(\frac{a}{D_{\rm eq}}\right)^{3/2}E_{\rm hp}. \tag{7.5}$$

As $E_{\rm ep}<W_L$, the polymer end-point E in the metastable state in Fig. 4(b), will more likely return to the medium [the situation in Fig. 4(a)] than to move to the unstable state in Fig. 4(c) that precedes the very annihilation event [Fig. 4(d)]. Overall, by Eq. (7.4), the displacement from the metastable state in Fig. 4(b) to the critical state in Fig. 4(c) is hindered by potentially large energy barrier W_L. In the case of sterically stabilized lyotropics, by Eqs. (7.4), (5.7), and (5.10), we have $W_L/k_BT\sim(E_{\rm hp}/k_BT)^{1/3}$, signaling substantial en-

ergy barriers in systems with high hairpin energies. For example, for the hairpin example discussed in sterically stabilized phases [see Eq. (5.16)] having $E_{\rm hp}=21.4\ k_BT$, by Eq. (7.4) we obtain $W_L\approx 3k_BT$. On the other hand, for the hairpin examples discussed in DNA-cationic lipid complexes in Sec. VI, Eq. (7.4) predicts a huge $W_L/k_BT\approx 15$. It should be stressed though that Eq. (7.4) is strictly valid only for large hairpins with $D_{\rm eq}\gg a$, whereas, as discussed in Sec. VI, one has $D_{\rm eq}\approx a$ in these complexes. Nonetheless, it is plausible that the Arrhenius factor $R_A=\exp(W_L/k_BT)$ is big for hairpins in these systems.

Potentially large energy barriers are not the only factor that may contribute to long lifetimes of hairpins in systems such as DNA-cationic lipid complexes. In fact, even without any energy barrier, it takes typically a long time for the annihilation in Fig. 4 to happen. The motion of polymer end points is mediated by slow reptational diffusion, and for typically long DNA molecules, it may take a substantial amount of time for the end-point E in Fig. 4, to reach close to the hairpin (even without trying to climb over any energy barrier). To illustrate this, let us consider a hairpin as in Fig. 4, folded on a λ-DNA molecule with $l=16\,000$ nm corresponding to $N=50\,000$ base pairs (as actually used in the experiments, [4]). For the reptation time needed for the end-point E to reach close to the hairpin in Fig. 4(a), we have

$$t_{\rm rep}\sim\frac{l^2}{D(N)}, \tag{7.6}$$

with $D(N)$, the reptational diffusion constant: $D(N)=D(1)/N$. Here, at most, $D(1)\sim 10^{-9}\ {\rm m^2\ s^{-1}}$, diffusion constant magnitude of nanometer size particles in water. With this, for the λ-DNA, we find $t_{\rm rep}\sim 10^4$ s. So, it may take few hours for the end-point E in Fig. 4(a) just to reach the hairpin void at the center of a λ-DNA molecule, before attempting to cross the potential barrier therein. As $t_{\rm rep}\sim N^3$, this reptation time scale is typically large for DNA molecules with a large number of base pairs $N\sim l$. This reptation time sets the minimum time scale for the life time of hairpins, that may be estimated as

$$t_{\rm hp}=t_{\rm rep}R_A, \tag{7.7}$$

where $R_A=\exp(W_L/k_BT)>1$ is the afforementioned Arrhenius factor associated with the energy barrier W_L in hairpin void area. As discussed above, it is plausible that R_A has a large value for hairpins in DNA-cationic lipid complexes. In fact, even with an energy barrier significantly smaller than the one anticipated above ($15\,k_BT$), such as $W_L=4\,k_BT$, one obtains by Eq. (7.7) a significant hairpin lifetime scale, $t_{\rm hp}\sim 10^6$ s, for the above example of λ−DNA molecules used in DNA-cationic lipid complexes. Likely, the actual hairpin lifetime scale in these systems is larger. Whatever is its value, the above simple estimates show that these systems are capable to maintain substantial nonequilibrium concentrations of hairpin dislocations over long times.

Finally, we note that there are other potentially interesting modes of hairpin extinction. An example is the annihilation of hairpin pairs folded on the same semiflexible polymer (unfolding process), see Appendix B and Fig. 5. As discussed in Appendix B, this process is typically much slower than the hairpin annihilations by polymer end-point dislocations discussed in this section.

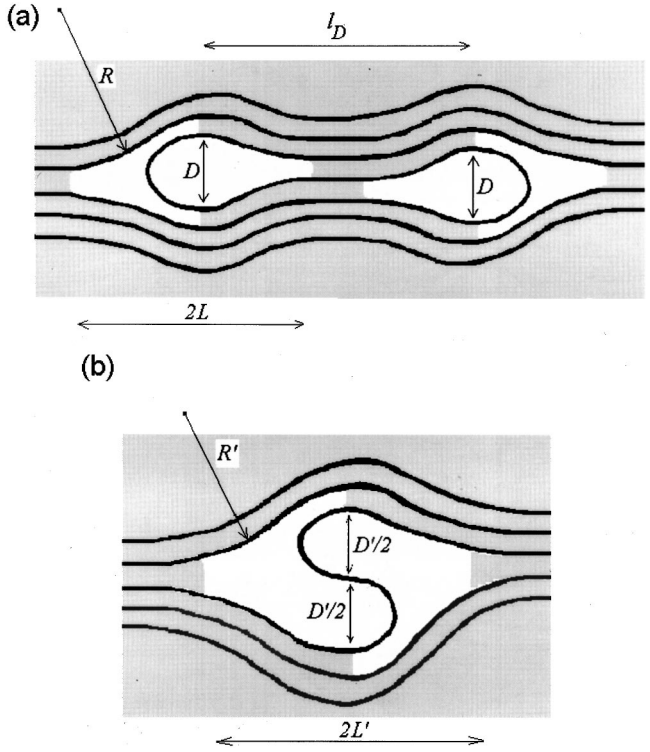

FIG. 5. Hairpin-hairpin annihilations in lyotropic 2D smectics. (a) Opposite hairpin dislocations folded on the same semiflexible polymer. (b) Unstable transition state with an *S*-shaped polymer section. It is the transition state (saddle point) between the dislocation pair state in (a) and a dislocation free state. Note that in this mode of annihilation, the hairpins need to perform the displacement l_D through the smectic medium before the nucleation in (b) may be attempted. This is in marked contrast to annihilations of hairpins by polymer end points, in which hairpins do not move (see Fig. 4).

VIII. SUMMARY

In this paper, we have elucidated phenomenology of hairpin-turn dislocations in 2D smectic phases of long semiflexible molecules. We have discussed hairpin dislocations shapes, sizes, and their free energies. We find that the hairpin turns may be, under some circumstances, substantially bigger than the smectic period size. Such hairpin turns are accompanied by large voids in the smectic medium. Hairpin voids are stable equilibrium structures with sizes determined by a competition between the polymer bending elasticity and smectic bulk elasticity. Hairpin dislocations with large voids are shown here to have relatively low free energies, significantly smaller than anticipated in earlier naive estimates.

Hairpin shapes, sizes, and energies are shown here to be qualitatively sensitive to the detailed nature of smectic materials. We have documented this by considering two major classes of smectics, thermotropic and lyotropic and lyotropic 2D smectics-*A*. We have considered typical thermotropic

smectics-*A* that are stable even at zero external isotropic pressure due to having intermolecular potentials with a minimum at a preferred distance between semiflexible polymers. In these materials, at zero pressure, interfaces between hairpin voids and the smectic medium are nearly straight lines. We have also considered hairpins in typical lyotropic smectics-*A*, stabilized by the repulsion between polymers causing a positive osmotic pressure. In these materials, the interfaces between hairpin voids and the smectic medium are nearly circular sections. For both the thermotropic and the lyotropic 2D smectics, we have obtained hairpin dislocation sizes and energies. These quantities were related to basic materials properties, such as the smectic penetration length λ, the size of the smectic phase period a, and the semiflexible polymer persistence length ξ_p. Qualitative forms of these relations are found to be different for lyotropic and thermotropic smectic materials.

We have applied our results for lyotropic smectics to entropically stabilized systems of long semiflexible polymers with purely hard-core repulsion that are 2D analogs of fluid membrane phases stabilized by steric entropy, [18,9–11]. In these systems, we have found that the hairpin dislocation size D is substantially bigger than the phase period a, for $a \ll \xi_p$. This expansion of the hairpin core into the surrounding smectic medium is associated with a significant reduction of hairpin dislocation energy. We have also discussed hairpin dislocations in quasi-2D smectics in DNA-cationic lipid complexes [4,5]. For hairpin dislocations in these systems, we find that $D \approx a$, whereas the hairpin dislocation energy is significantly bigger than $k_B T$. Under realistic experimental conditions, we expect no hairpin dislocations to be observable in these systems *if* they would be in true thermodynamic equilibrium. Nonetheless, these systems are capable to maintain, over long time scales, large initial nonequilibrium concentrations of hairpin dislocations, possibly created in the early stage of the formation of DNA-cationic lipid complexes by mixing. In these systems, the extinction of hairpin dislocations goes on by their annihilations with polymer end points. The rate of this process is shown to be hindered by sluggish reptational diffusion of DNA molecules, as well as by substantial energy barriers.

ACKNOWLEDGMENTS

I thank Tim Salditt and Joachim Raedler for discussions on DNA-cationic lipid complexes, and John Toner for a helpful remark. This research has been supported in part by grants from the Eberly College of Arts and Sciences, and from the Los Alamos National Laboratory (CNLS) operated by DOE. This research has been carried out in part at Harvard University. I would like to thank the Harvard University physics department, in particular, Professor David Nelson for his kind hospitality and generous support.

APPENDIX A

In this appendix, we discuss two different ways to derive equilibrium shapes of semiflexible polymers: the grand-canonical (fixed chemical potential) description in Eqs. (3.2), and (3.3), and the canonical (fixed polymer length) description in Eqs. (3.4) and (3.5). Also, we discuss the equivalence conditions for the two descriptions stated in Eq. (3.6).

We first briefly outline derivations of these two descriptions. The grand-canonical ensemble description in Eq. (3.2) may be derived by considering the grand-canonical free-energy Eq. (3.1) in the so-called Monge parametrization, in which the polymer shape in the (x,z) plane is specified by giving, e.g., x as a function of z, that is, $x=f(z)$. By noting that $ds=dz\sqrt{1+(df/dz)^2}$, Eq. (3.1) becomes, in the Monge parametrization,

$$G_{\rm turn}(f)=\int dz\,\sqrt{1+\left(\frac{df}{dz}\right)^2}\left[-\mu+\frac{\kappa H^2}{2}\right], \qquad \text{(A1)}$$

with

$$H=\frac{d}{dz}\left[\frac{df/dz}{\sqrt{1+\left(\frac{df}{dz}\right)^2}}\right],$$

the polymer curvature. Applying the variational condition $\delta G_{\rm turn}/\delta f(z)=0$, yields a long and fairly complicated differential equation for $f(z)$. That equation turns out to be equivalent to our simple equation (3.2), as may be verified by expressing Eq. (3.2) in the Monge parametrization, by expressing d/ds as $[1+(df/dz)^2]^{-1/2}d/dx$.

Next, we briefly discuss the canonical ensemble description in Eq. (3.4). This sine-Gordon-type equation appears in the *Elastica* problem of a flexible rod bent in the (x,z) plane under a force $\mathbf{F}=(F_x,F_z)=F[\sin(\phi_0),\cos(\phi_0)]$ acting on its end [25]. The rod's equilibrium shape may be obtained by varying over $\phi(s)$ the functional,

$$\begin{aligned}\tilde{E}(\phi)&=E_{\rm bend}-F_x x(l)-F_z z(l)\\&=\int_0^l ds\left\{\frac{\kappa}{2}\left(\frac{d\phi}{ds}\right)^2-F_x\sin[\phi(s)]-F_z\cos[\phi(s)]\right\}.\end{aligned} \qquad \text{(A2)}$$

This yields an equation identical to Eq. (3.4) with $\Lambda=-F$. Thus, the parameter Λ of Sec. III is essentially the reaction force of the rod. Applied to our problem, this means that Λ is the force exerted by the polymer turn in Figs. 1 and 2 onto the surrounding smectic medium. This is exemplified by the equation (3.18) of the Sec. III.

Finally, we proceed to derive Eq. (3.6) relating the grand-canonical and canonical description. By the canonical description Eq. (3.4), we have

$$\phi(s)=\phi_0+\cos^{-1}[Q(s)], \qquad \text{(A3)}$$

where $\cos^{-1}$ signifies the inverse-cosine function, and

$$Q(s)=\frac{\frac{1}{2}\kappa H^2-C_\phi}{\Lambda}. \qquad \text{(A4)}$$

Differentiating Eq. (A3) with respect to s, and squaring the resulting equation, yields

$$H^2=\frac{\left(\frac{dQ}{ds}\right)^2}{1-Q^2}. \tag{A5}$$

Inserting into Eq. (A5) the quantity $Q(s)$ defined by Eq. (A4), yields the equation

$$-\frac{C_\phi}{2}H^2+\frac{\kappa}{8}H^4+\frac{\kappa}{2}\left(\frac{dH}{ds}\right)^2=\frac{\Lambda^2-C_\phi^2}{2\kappa}. \tag{A6}$$

It is easy to see that Eq. (A6) is identical to the grand-canonical ensemble Equation (3.3), provided the canonical parameters Λ and C_ϕ are related to grand-canonical ensemble parameters μ and C_H in the way we stated in the equation Eq. (3.6). Q.E.D.

It should be noted that the relation in Eq. (3.6) between the two descriptions is not a simple one. For example, it may be naive to expect that one may directly relate the major parameter of the canonical description, the reaction force Λ, to the major parameter of the grand-canonical description, the chemical potential μ. However, by Eq. (3.6), the relationship is not so simple. For example, the value of Λ depends not only on μ but also on the value of the integration constant C_H, which is yet another parameter of polymer shape solutions obtained by the grand-canonical description.

APPENDIX B

As noted in Sec. VII, a potentially interesting mode of hairpin extinction in 2D smectics is annihilation of hairpins pairs folded on the same semiflexible polymer (unfolding process), see Fig. 5. Consider a pair of opposite hairpin dislocations folded on the same semiflexible polymer depicted in Fig. 5(a). For them, thermal fluctuations may activate an unstable transition state incorporating an *S*-shaped polymer section depicted in Fig. 5(b). Such a state is the transition state (saddle point) between the dislocation pair state in Fig. 5(a) and a dislocation free state. The activation energy of the transition state is

$$E_A=E'-2E_{\rm hp}. \tag{B1}$$

Here, E' is the free energy of the transition state in Fig. 5(b), whereas $E_{\rm hp}$ is single hairpin dislocation free energy. E_A in Eq. (B1) is thus the energy barrier between the dislocation pair state [Fig. 5(a)] and a dislocation free state. The activation barrier E_A limits the rate of hairpin pairs annihilations.

Transition state energy E' may be calculated along the lines similar to those we used to find $E_{\rm hp}$ in this paper. A major difference between the transition state [Fig. 5(b)] and a single hairpin dislocation state (Fig. 1), is in the shape of the polymer section in the center of these deffects. For the dislocation case, it is a *C*-shaped section discussed in Sec. III (see Fig. 2 therein). On the other hand, for the case of the transition state, we have an *S*-shaped polymer section, see Fig. 5(b). Its shape is determined by the same equation we used in Sec. III to find the shape of the *C*-shaped polymer turn [see Eq. (3.11)]. In fact, as already noted in Sec. III, this equation yields a periodic *Elastica* curve for the polymer shape, see Fig. 2(b). *C*-shaped polymer turns correspond to one-half of the curve's period, whereas the *S*-shaped sections correspond to one full period of the *same* curve. This full period fills the smectic medium opening with the vertical size D' indicated in Fig. 5(b). As the *S*-shaped section is actually composed of *two* *C*-shaped sections each having vertical size $D'/2$, its energy is, by Eq. (3.17),

$$E_S(D')=2\left(2C^2\frac{\kappa}{D'/2}\right)=2(2C)^2\frac{\kappa}{D'}. \tag{B2}$$

Note that the Equation (B2) for the *S*-section energy is isomorphic to Eq. (3.17) for the *C*-section energy, provided the constant C therein is replaced by

$$C'=2C. \tag{B3}$$

Having the *S*-section energy in Eq. (B2), the vertical size D', and energy E' of the transition state may be determined along the same lines we used in Sec. IV to find the size D and energy $E_{\rm hp}$ of hairpin dislocations. Thus, we have

$$E'=2F_w(D')+2(C')^2\frac{\kappa}{D'}, \tag{B4}$$

where the first the term is the smectic medium contribution to E'. Notably, Eq. (B4) is isomorphic to the Eq. (4.1) for hairpin dislocation energy, provided $E_{\rm hp}$, D, and C therein are replaced by E', D', and $C'=2C$, respectively. This isomorphism may be used to find E' and D' in a quick way. These quantities may be obtained simply by replacing $E_{\rm hp}$, D, and C in various results of Sec. IV, by E', D', and $C'=2C$, respectively. Thus, by Eqs. (4.3) [or (4.7)], (4.4) [or (4.8)], and (4.9), with $C\to C'=2C$, we find, for the transition state in lyotropic smectics,

$$D'=2^{4/5}D_{\rm eq},\quad L'=2^{2/5}L_{\rm eq},\quad R'=R. \tag{B5}$$

Equation (B5) relates the geometrical sizes of the transition state, depicted in Fig. 5(b), to those of hairpin dislocations in the *same* material. Likewise, by Eq. (4.5), with $C\to C'=2C$,

$$E'=2^{6/5}E_{\rm hp}. \tag{B6}$$

Equation (B6) relates energy of the transition state in Fig. 5b to the equilibrium energy of a single hairpin dislocation in the same lyotropic material. Like to their dislocation counterparts of Sec. IV, relations in Eqs. (B5) and (B6) are exact in the situations with $D_{\rm eq}\gg a$ and may be used to make sound estimates even in situations with $D\sim a$.

By Eq. (B6), the activation energy for annihilations of hairpin dislocation pairs in lyotropic materials, Eq. (B1), is

$$E_A=(2^{6/5}-2)E_{\rm hp}\approx 0.2974\ \ E_{\rm hp}. \tag{B7}$$

Thus, the pair annihilation activation energy E_A is simply proportional to hairpin dislocation energy. By comparing Eq.

(B7) with the energy barrier for the hairpin annihilations with end-point dislocations W_L [see Eq. (7.4)], we see that

$$W_L \approx 1.0091 \frac{a}{D_{\rm eq}} E_A . \tag{B8}$$

Thus, $W_L < E_A$, in the situations with $D_{\rm eq} > a$ (at least). Thus, hairpin-hairpin annihilations are hindered by energy barriers larger than those for hairpin annihilations by polymer end points. Another factor making hairpin-hairpin annihilations less significant for extinction of hairpins, are potentially long times needed for two hairpins to approach each other before attempting to annihilate. Note that in the hairpin-hairpin mode of annihilation, distant hairpins need to execute the displacement l_D through the smectic medium [see Fig. 5(a)] before the nucleation in Fig. 5(b) may be attempted. The sole time needed for this displacement to occur will be thus large in the situations with large separations between hairpins. This is in marked contrast to annihilations of hairpins by polymer end points, in which hairpins do not move *at all* through the smectic medium, see Sec. VII. This process is mediated by polymer reptation, which does not displace hairpins, and thus, does not cause significant displacement in the surrounding smectic medium (see Fig. 4). On the other hand, motion of large hairpins in Fig. 5 is a substantially slower process, as it requires large displacements of the surrounding smectic medium.

Obviously, hairpin-hairpin annihilations will be significant in the situations in which there are many hairpins folded on the same polymer. For the case of hairpins with very large energies, such a state may be realized only in situations that are very far from equilibrium. For semiflexible polymers of a finite length, a more typical nonequilibrium state is that with a single hairpin folded on a polymer (as in Fig. 4). For these more typical nonequilibrium situations, the only mode of hairpin extinction is by their annihilations with polymer end points, as described in Sec. VII.

[1] J. Toner and D. R. Nelson, Phys. Rev. B **23**, 316 (1981).

[2] L. Golubović and Z.-G. Wang, Phys. Rev. Lett. **69**, 2535 (1992); Phys. Rev. E **49**, 2567 (1994).

[3] J. O. Raedler, I. Koltover, T. Saldit, and C. R. Safinya, Science **275**, 810 (1997).

[4] T. Salditt, I. Koltover, J. O. Raedler, and C. R. Safinya, Phys. Rev. Lett. **79**, 2582 (1997); Phys. Rev. E **58**, 889 (1998).

[5] F. Artzner, R. Zantl, G. Rapp, and J. O. Raedler, Phys. Rev. Lett. **81**, 5015 (1998); R. Zantl, F. Artzner, G. Rapp, and J. O. Raedler, Europhys. Lett. **45**, 90 (1998).

[6] L. Golubović and M. Golubović, Phys. Rev. Lett. **80**, 4341 (1998); **81**, 5704(E) (1998).

[7] C. S. O'Hern and T. C. Lubensky, Phys. Rev. Lett. **80**, 4345 (1998).

[8] L. Golubović, T. C. Lubensky, and C. S. O'Hern, Phys. Rev. E **62**, 1069 (2000).

[9] F. C. Larche, J. Appel, G. Porte, P. Bassereau, and J. Marignan, Phys. Rev. Lett. **56**, 1700 (1986).

[10] C. R. Safinya, D. Roux, G. S. Smith, S. K. Sinha, P. Dimon, N. A. Clark, and A. M. Belocq, Phys. Rev. Lett. **57**, 2718 (1986). See, also, D. Roux and C. R. Safinya, J. Phys. (Paris) **49**, 307 (1988).

[11] L. Golubović and T. C. Lubensky, Phys. Rev. B **39**, 12 110 (1989).

[12] N. Lei, C. R. Safinya, and R. F. Bruinsma, J. Phys. II **16**, 299 (1995).

[13] R. Holyst, Phys. Rev. A **42**, 7511 (1990); R. Holyst, D. J. Tweet, and L. B. Sorensen, Phys. Rev. Lett. **65**, 2153 (1990).

[14] P. G. de Gennes, Europhys. Lett. **13**, 709 (1990).

[15] T. Odijk, Macromolecules **19**, 2313 (1986).

[16] M. Dijkstra, D. Frenkel, and H. N. W. Lekkerkerker, Physica A **193**, 374 (1993).

[17] T. W. Burkhardt, J. Phys. A **30**, L167 (1997).

[18] W. Helfrich, Z. Naturforsch. Teil A **33**, 305 (1978); W. Helfrich and R. M. Servus, Nuovo Cimento D **3**, 137 (1984).

[19] P. G. de Gennes and J. Prost, *Physics of Liquid Crystals* (Oxford University Press, Oxford, 1993). We note that Eq. (2.1) is obtained from the smectic harmonic elasticity model. It ignores elastic nonlinearities producing an anomalous behavior of 2D smectic elastic constants at long length scales, see Ref. [2]. As noted in Sec. IV, these effects are not substantial here as the anomalous Ginzburg length scales exceed hairpin sizes. Besides, interestingly, these anomalous effects are presumably exactly canceled due to a special feature of the 2D smectic anharmonic elasticity: The product $K_{\rm sm}B_{\rm sm}$, entering $\delta\gamma$ in Eq. (2.1) turns out *not* to be renormalized at long length scales, as found in Ref. [2] by an exact mapping of 2D smectics onto the Kardar-Parisi-Zhang model.

[20] The quantity γ_0 of Ref. [14] is to be properly identified as *one half* of the thermotropic smectic binding energy $|V(a)|$, i.e., in our case, binding energy per unit length of a pair of long semiflexible polymers.

[21] L. D. Landau and E. M. Lifshitz, *Theory of Elasticity* (Pergamon, New York, 1986).

[22] L. Golubović and S. Feng, Phys. Rev. A **43**, 5223 (1991); L. Golubović and A. Peredera, Phys. Rev. E **51**, 2799 (1995).

[23] L. Golubović and T. C. Lubensky, Phys. Rev. A **41**, 4343 (1990).

[24] L. Golubović, Phys. Rev. E **50**, R2419 (1994).

[25] A. E. Love, *A Treatise on the Mathematical Theory of Elasticity* (Dover, New York, 1994).

[26] L. D. Landau and E. M. Lifshitz, *Statistical Physics* (Pergamon, Oxford, 1969)

[27] P. G. de Gennes and C. Taupin, J. Phys. C **86**, 2294 (1982).

[28] S. A. Safran, D. Roux, M. E. Cates, and D. Andelman, Phys. Rev. Lett. **57**, 491 (1986).

[29] D. Morse, Phys. Rev. E **50**, R2423 (1994).

[30] L. Golubović (unpublished).

[31] More recent experiments of Raedler and co-workers on oriented samples of DNA-cationic lipid complexes (see Ref. [5]), indicate the existence of such a nematic phase; J. Raedler (private communication).